Ocean Engineering 296 (2024) 117033

Contents lists available at ScienceDirect

Ocean Engineering

journal homepage: www.elsevier.com/locate/oceaneng

Collaborative matching design method of lifting trajectory and ballast water allocation for revolving floating cranes with experimental validation

Xiaobang Wang [a,b], Siyu Li [a,b], Yang Yu [a,b], Jie Zhang [c], Zhijie Liu [a,b,*]

[a] Naval Architecture and Ocean Engineering College, Dalian Maritime University, Dalian 116026, China
[b] Key Laboratory for Polar Safety Assurance Technology and Equipment of Liaoning Province, Dalian 116026, China
[c] The University of Texas at Dallas, Richardson, TX 75080, USA

ARTICLE INFO

Keywords:
Collaborative matching design
Revolving floating crane
PTP theory
Trajectory planning
Ballast water allocation

ABSTRACT

The Revolving FloatingCrane (RFC) is a vital engineering vessel for offshore lifting operations, with its operational safety and stability being of utmost importance. Nevertheless, potential mismatches in the lifting trajectory and ballast water allocation during manual operations may result in low efficiency, instability, and energy dissipation. Thus, a novel collaborative matching design (CMD) method of the lifting trajectory and ballast water allocation is proposed for the RFC intelligence. By establishing one-to-one correspondences between the lifting trajectory and the ballast water allocation, the CMD method is first developed based on the point to point (PTP) theory. Then, the dynamics model of lifting operations and CMD optimization model are established. To explore the superiority, the proposed CMD method is compared with the conventional method, finding that the CMD method surpasses the conventional sequential design method in terms of lifting operation time (11.20% reduction), total energy consumption (16.50% reduction), ballast water allocation (17.84% reduction), and decision-making time (54.50% reduction). Finally, numerical and experimental validations regarding various lifting scenarios are conducted to certify the efficacy and feasibility of the proposed CMD method, underscoring its potential to realize the optimal matches between RFC's lifting trajectory and ballast water allocation.

1. Introduction

The abundant marine resources have gradually attracted a lot of attentions fro relevant fields, and the revolving floating crane (RFC), with its strong lifting capacity, outstanding environmental adaptability and deep-sea operation capability, has gradually become the core equipment of major offshore operations, including offshore lifting, maritime rescue, deep-sea salvage, offshore platform construction, etc. Wilson (2003). The specific structure of RFC is illustrated in Fig. 1, which mainly consists of the lifting system above the deck and the ballast system in the hold. As a huge and complex engineering machinery, the safety and stability of RFC offshore operations are crucial, directly determining the implementation safety of the entire offshore project (Gunnu and Moan, 2018). However, due to the enormous lifting weight, RFC is susceptible to lateral tilting due to the overturning torque during lifting operations and the ballast system is used to ensure the balance of the vessel. Obviously, the collaboration between the lifting system and the ballast system is crucial in RFC offshore lifting operations.

Currently, actual offshore lifting operations, including lifting activities (based on the planned trajectory) and ballast water allocation, rely entirely on the coordination between the crane operators and the chief mate based on their professional knowledge and operational experience. This manual collaborative operation method is easily affected by factors such as personnel status, sea conditions, and weather situations, resulting in long decision-making time, high energy consumption, and low work efficiency, which may seriously affect the quality and safety of the entire offshore operations. For the above issues, the intelligent upgrade of the RFC is an effective solution, and the key to intelligent operations lies in the reasonable matching between the lifting trajectory and the ballast water allocation of the RFC. Therefore, a collaborative matching design (CMD) method for the lifting trajectory and the ballast water allocation of the RFC is urgently needed.

Ballast water allocation optimization has emerged as a research hotspot in recent years, driven by the trend towards greater intelligence in the operation of the RFC. Liu et al. (2022a,b) adopted the dynamic programming method to optimize the ballast water allocation for the RFC ballast system, aiming to enhance the operational efficiency, and obtained results indicated that the established method can reliably improve the ballasting performance. Jia and Lei (2021) established a

* Corresponding author at: Naval Architecture and Ocean Engineering College, Dalian Maritime University, Dalian 116026, China.
E-mail addresses: wxb@dlmu.edu.cn (X. Wang), liuzj@dlmu.edu.cn (Z. Liu).

https://doi.org/10.1016/j.oceaneng.2024.117033
Received 22 October 2023; Received in revised form 19 January 2024; Accepted 4 February 2024

Fig. 1. The specific structures of the RFC (CRS, 2011).

ballast water allocation optimization model following a multiobjective evolutionary algorithm based on decomposition (MOEA/D), results showing that the number of ballast tanks involved in ballast adjustment is reduced to some extent. Rethfeldt et al. (2023) developed an allocation algorithm inspired by optimization-based solutions known from dynamically positioning ships, simulation processes obtaining the promising results. Chen et al. (2023) applied the fuzzy analytical hierarchy process (FAHP) to set up two decision support frameworks for the ballast water allocation, and results showed the effectiveness of the assessment criteria of the framework. Wang et al. (2022a) developed a novel sequential matching optimization (SMO) method for the ballast water allocation and the lifting trajectory of the RFC, numerical experiments verifying the corresponding feasibility. Wang et al. (2022b) introduced a dynamic programming-based approach for optimizing the ballast water allocation of the underwater robot, which is potentially applicable to RFC ballast water allocation. Simulation results demonstrated that the proposed approach can effectively reduce the ballast time. Guo et al. (2021) developed an Integrated Scheduling Model (ISM) that coordinates both vessel scheduling and ballasting operations. Extensive experimentation demonstrated the significant role of ISM in enhancing port efficiency. Zhu et al. (2020) devised a novel ballast strategy grounded in global optimization for dynamic ballast water allocation. Results indicated that the optimization solutions can supplement the current analysis workflow and aid engineers in decision-making processes. Liu et al. (2018) introduced an efficiency-focused optimization model of ballast water allocation for the RFC, with the objective of minimizing both the volume of ballast water and the allocation time, finding that this optimized approach outperforms traditional ballast water allocation methods. Chen et al. (2010a,b) created an optimization model to streamline large-scale sequential ballast water exchange, utilizing a multi-objective genetic algorithm. A case study on an 176,000 DWT bulk carrier confirmed the model effectiveness. Kurniawan and Ma (2009) utilized a multi-objective evolutionary algorithm to optimize the ballast water allocation, aiming at increasing the ballast allocation efficiency. Numerical evaluations suggested that this approach surpasses the conventional method.

For trajectory planning methods of crane lifting operations, the quality directly influences the performance of the intelligent lifting procedure of the entire RFC and relevant research has been carried out in this aspect. Lu et al. (2022) proposed an online method for planning three-dimensional trajectories of offshore cranes, which demonstrated high accuracy in cargo delivery in simulations. Huang et al. (2020) introduced an intelligent trajectory planning method for tower crane lifting tasks under complex working conditions, and the optimization process demonstrated high computational performance. Tho et al. (2020) presented a simple trajectory planning method for an overhead crane using S-curve, and both simulation and experimental results are given to verify the effectiveness of the proposed method. Peng et al. (2019) developed a trajectory planning approach for bridge cranes, designed to boost precision and safety in lifting operations. Simulation outcomes affirmed the viability of the proposed approach. Liong et al. (2023) used the Long Short Term Memory (LSTM) to approximate working trajectories of robotic arms, finding that it can enhance productivity and promote worker safety. Li et al. (2023a) proposed a kinematic coupling-based trajectory planning method for double-pendulum rotary cranes. Numerical simulation and real experiments verified the robustness of the proposed method. Dutta et al. (2023) introduced a multi-objective anti-swing trajectory planning method for tower cranes, simulated trajectories demonstrating that the proposed method can produce time-energy optimal solutions. Fang et al. (2019) devised an S-curve trajectory planning method for industrial robots, proving its efficiency and practicality through simulations and experiments. Rams et al. (2017) developed a trajectory optimization methodology using flatness-based and energy-based feedback for single mast stacker cranes. The applicability of this approach were substantiated through experimental results. Hoang et al. (2014) introduced an offline crane trajectory planning method that effectively lessened payload swing, with simulations confirming its effectiveness and tracking precision.

As seen from the above work, there has been certain research in the fields of the ballast water allocation optimization and the trajectory planning, respectively. Currently in the field of ballast water allocation optimization, most research only unilaterally focuses on the decision for ballast water allocation, without considering the impacts of the lifting trajectory on the ballasting process. Similarly, while performing the trajectory planning for the RFC crane, the ballast water allocation is always ignored. Essentially, strong coupling effects exist between the lifting trajectory and the ballast water allocation of the RFC, however, there is little literature focusing on this issue. Although some researchers have acknowledged this issue and suggested a sequential design (SD) method (Wang et al., 2022a; Chen et al., 2010a), in which the trajectory is determined first, followed by the ballast plan, this method maintains a separation between trajectory planning and ballast water allocation. Such segregation can result in an inconsistency between the “optimal” lifting trajectory and the “optimal” ballast scheme, thereby diminishing rather than improving the comprehensive operational performance of the RFC with notable decreases in safety, energy efficiency, and operational efficiency, as depicted in Fig. 2. Consequently, the existed sequential design method also fails to yield a truly optimal lifting solution. To genuinely realize intelligent offshore lifting operations for the RFC, the collaborative matching between these two aspects cannot be overlooked. Given the foregoing, there is a pressing need to propose a collaborative matching design (CMD) method of lifting trajectory and ballast water allocation for the RFC. This method would synchronize trajectory planning and ballast water allocation optimization, thereby enabling the resolution of a truly optimal solution for maritime lifting operations.

The remaining of this study is organized as follows. Section 2 introduces the CMD method of the lifting trajectory and the ballast water allocation for the RFC. Section 3 establishes the optimization model of the CMD method of the lifting trajectory and the ballast water allocation. In Section 4, the feasibility of the CMD method is demonstrated by a practical case study, and its superiority is proved by comparison with conventional design methods. In Section 5, the effectiveness of the CMD method is further validated through actual experiment studies under a variety of different working conditions. Section 6 provides the concluding remarks and future work.

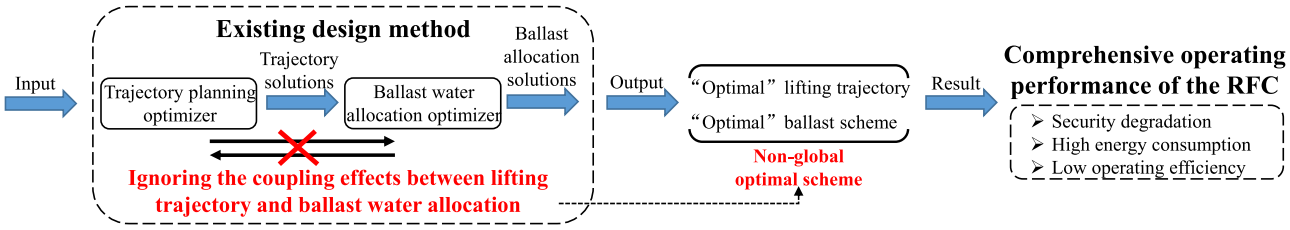

Fig. 2. The existing design issues in RFC offshore lifting operations.

2. CMD method of RFC lifting trajectory and ballast water allocation

2.1. The intelligent operation process of the RFC

As illustrated in Fig. 1, the structures of the RFC comprise the crane on the upper level and the ballast system inside. The crane is responsible for carrying out lifting activities, directly interacting with the cargo. It accomplishes the movement of the cargo through a base with rotating motion, a variable amplitude boom with adjustable span, and a hoisting cable for lifting operations. The ballast system, composed of ballast pumps, ballast tanks, hydraulic valves, pipelines, and other components, aims to inject an appropriate amount of seawater into the ballast tanks to adjust the RFC's draft and stability.

The offshore lifting operation of the RFC is a complex process with multiple stages. Fig. 3 displays the entire lifting process of the intelligent RFC. Firstly, it is necessary to determine relevant information about the lifting task, such as the lifting load, and the starting and target positions of the lifting operation. Based on the lifting task requirements, the intelligent lifting operation scheme is determined by adopting relevant intelligent solving methods. The next step is the preparatory stage before the lifting activities, during which the RFC begins to pre-ballast. While the crane arm is arriving at the initial lifting position, the ballast system is injecting enough ballast water into the tanks to prevent the hull from becoming unbalanced after suddenly loading a heavy mass. Then, during the offshore operation stage, the loading mass is lifted along the predetermined trajectory, while a corresponding ballast scheme is executed by the ballast system based on the real-time position of the loading mass to maintain hull balance. Throughout the lifting operation, it is essential to monitor in real-time whether the hull is in a safe state. If unexpected circumstances occur (such as severe sea conditions, sudden system failures, or lack of synchronization between the crane and ballast system), the lifting operation is immediately suspended, and an emergency plan is executed for urgent risk avoidance. If no sudden situations occur during the lifting operation, the lifting operation will proceed as planned. During the procedural lifting operation, the monitoring system constantly monitors whether the loading mass has reached the target position. If the loading mass reaches the target position, the lifting operation is completed; if not, the lifting operation will continue.

Through the observation of the entire process illustrated in Fig. 3, it is noticed that the safety and stability of the RFC throughout the lifting process highly depend on the degree of match between the lifting trajectory and the ballast water allocation. However, current trajectory planning and ballast water allocation processes largely rely on manual decision-making. Due to the considerable randomness of manual operations, it is difficult to accurately formulate an optimal lifting plan that simultaneously takes into account safety, efficiency, and energy saving. The CMD method of lifting trajectory and ballast water allocation for the RFC proposed in this study is the key to overcoming this predicament.

2.2. Point to point theory

Before diving into the specifics of the CMD method, it is first necessary to analyze the Point to Point (PTP) theory, a critical concept applied within this method. The PTP theory, conceptually grounded on high-order polynomials, is skillfully designed to tackle intricate optimal control problems (Huang et al., 2011; Hsu et al., 2014). This theory is adept at complying with constraints imposed on displacement, velocity, and acceleration at any moment. Mathematically, the objective is to identify corresponding functions for displacement, velocity, and acceleration, that is:

$$\begin{cases} v = v(t) \\ \dot{v} = \dot{v}(t) \\ \ddot{v} = \ddot{v}(t) \end{cases} \qquad t \in [t_i, t_f] \tag{1}$$

where, t denotes the time, with i and f representing the initial and final instances, respectively. $v(t)$, $\dot{v}(t)$, and $\ddot{v}(t)$ denote displacement, velocity, and acceleration, respectively. In the PTP theory, the displacement $v(t)$ of the dynamic system is characterized by a polynomial function. The velocity $\dot{v}(t)$ and the acceleration $\ddot{v}(t)$ are subsequently derived as below:

$$\begin{cases} v(t) = b_0 + b_1 t + b_2 t^2 + \cdots + b_{n-1} t^{n-1} + b_n t^n \\ \dot{v}(t) = b_1 + 2b_2 t + 3b_3 t^2 + \cdots + (n-1) b_{n-1} t^{n-2} \\ \qquad + n b_n t^{n-1} \\ \ddot{v}(t) = 2b_2 + 6b_3 t + 12 b_4 t^2 + \cdots + (n-1)(n-2) \\ \qquad b_{n-1} t^{n-3} + n(n-1) b_n t^{n-2} \end{cases} \tag{2}$$

where, b_n are coefficients of the polynomial, and n is a positive integer representing the polynomial degree.

Typically, the system initiates from a state of rest and stops at a distinct final position. Hence, at the initial instant, the imposed motion constraints on the system are:

$$v(t_i) = d_0 = 0; \quad v(t_f) = \kappa \tag{3}$$

$$\dot{v}(t_i) = d_1 = 0; \quad \dot{v}(t_f) = 0 \tag{4}$$

$$\ddot{v}(t_i) = d_2 = 0; \quad \ddot{v}(t_f) = 0 \tag{5}$$

where, κ represents the displacement at the final instant. At this point, by substituting Eqs. (3)~(5) into Eq. (2), the expressions of the polynomial coefficients b_3, b_4, and b_5 can be determined:

$$\begin{cases} b_3 = \dfrac{10\kappa}{T^3} - T^3 b_6 - 3T^4 b_7 - 6T^5 b_8 - 10T^6 b_9 \cdots \\ b_4 = -\dfrac{15\kappa}{T^4} + 3T^2 b_6 + 8T^3 b_7 + 15T^4 b_8 + 24T^5 b_9 \cdots \\ b_5 = \dfrac{6\kappa}{T^5} - 3T b_6 - 6T^2 b_7 - 10T^3 b_8 - 15T^4 b_9 \cdots \end{cases} \tag{6}$$

From the aforementioned derivations, it is apparent that the essence of the PTP theory is to translate the optimal control problem of solving differential equations of displacement, velocity, and acceleration for a dynamic system into a nonlinear constraint problem of determining the corresponding high-order polynomial coefficients (Wang et al., 2018). Once these coefficients are determined, the displacement, velocity, and acceleration of the dynamic system at any given instant can be acquired.

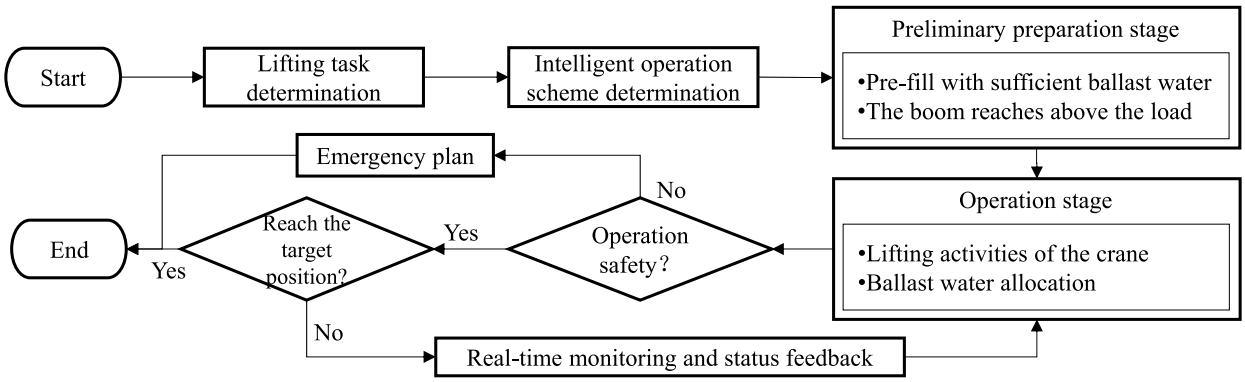

Fig. 3. The flow chart of the entire lifting process of the intelligent RFC.

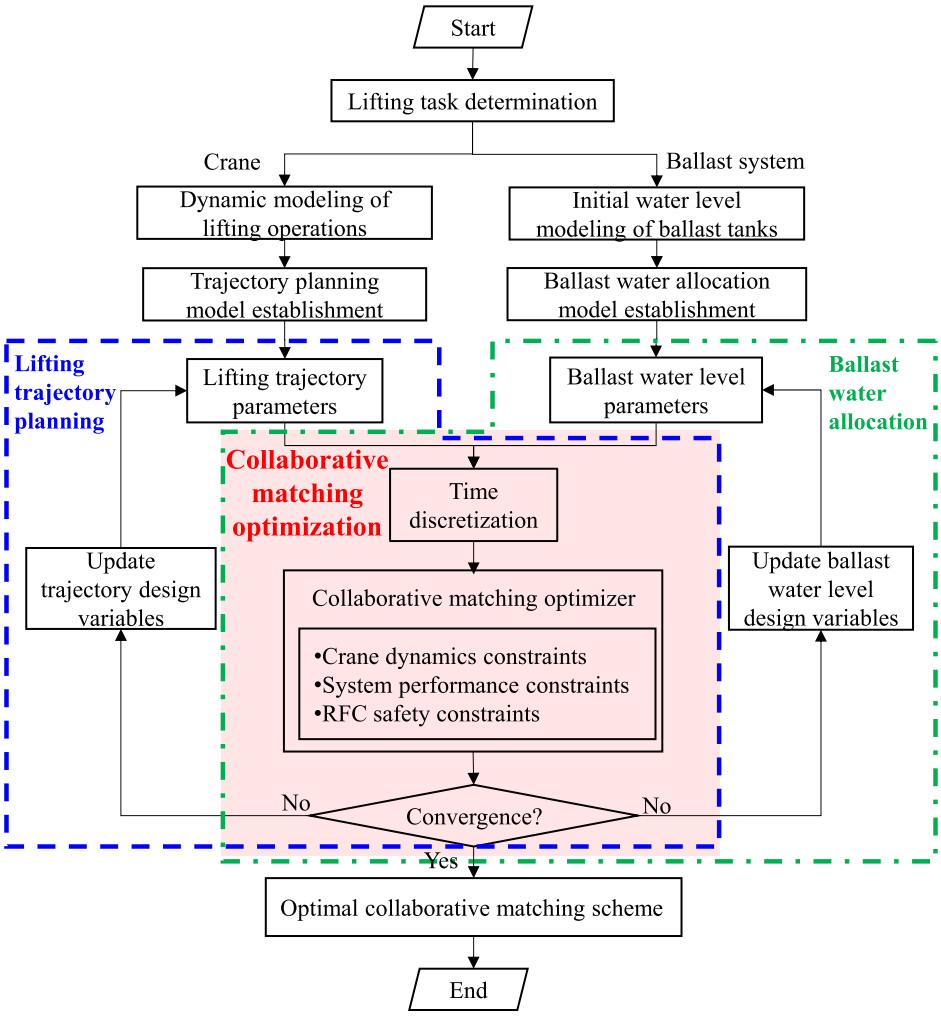

Fig. 4. The framework of the CMD method.

2.3. The CMD method for the intelligent RFC

Upon an in-depth understanding of the PTP theory, its applications are proved to be quite fitting for both the trajectory planning and the ballast water allocation optimization for the RFC. The trajectory planning essentially involves the optimal control of the crane lifting activities, from a specific initial point to a final destination point, given constraints on the displacement, velocity, and acceleration. Similarly, the optimization problem concerning ballast water allocation is also situated within the scope of the PTP theory. The objective here is to optimally control the allocation of ballast water from the initial time to the final time to maintain the balance and stability of the RFC.

At this point, the PTP-based CMD method of the lifting trajectory planning and the ballast water allocation for the RFC can be established. Fig. 4 illustrates the comprehensive framework for the established CMD method:

Table 1
The pseudocodes of solution process of the CMD method.

The CMD method of the lifting trajectory and the ballast water allocation
1: Determining the design variables and the corresponding ranges
2: Initializing the design variables
3: **while** (The iteration residual < the residual standard value) or (the iterations < the maximum allowed iterations)
4: Constructing the lifting trajectory intermediate model and the ballast water allocation intermediate model
5: Performing meticulous discretization throughout the entire time domain
6: Identifying the CMD goal and carrying out the optimization iteration
7: Updating design variables of the trajectory planning and water levels
8: **end while**

(i) Determine the details of the RFC offshore lifting task, including information on the starting and ending positions of lifting, the lifting load, the sea conditions, and the weather conditions.

(ii) Establish performance models for both the crane lifting operations and the ballast allocation operations. The performance model of the crane lifting operations includes the system dynamics model, the trajectory planning model, etc. The performance models of ballast allocation operations include the water level model of ballast tanks, the ballast water allocation model, etc.

(iii) Discretize the entire time domain to establish one-to-one correspondences between the lifting trajectory position coordinates and the water level in each ballast tank.

(iv) After fully considering the constraints regarding the lifting operation safety, the crane dynamics and the ballast system performance, the CMD model of the RFC is established. Then, it is necessary to select a reasonable intelligent optimization algorithm and execute iterative optimization solution;

(v) If the solution converges, output the optimal collaborative operation scheme of the lifting trajectory and the ballast water allocation. If not, update the design variables and continue with the iterative optimization solution.

2.4. Solution strategy for CMD method based on discretization idea

The CMD of RFC lifting trajectory and ballast water allocation is a dynamic and continuous decision-making process. Its degree of matching at any time depends not only on the current lifting trajectory position and water levels of each ballast tank, but also affects subsequent trajectory planning and ballast water allocation. Conventional solution strategies have limitations in dealing with the above dynamic and continuous issues and cannot realize the CMD of the RFC, so a continuous and matching solution strategy for the CMD method based on discretization idea is proposed.

As analyzed above, intermediate prediction models of the lifting trajectory and the water levels of each tank at any time of the operations are established based on the PTP theory, making the lifting trajectory and water levels to be solved and known at any optimization iteration process. To realize the continuous and matching solution procedure, it is crucial to meticulously discretize the whole operation time domain regarding the lifting trajectory and ballast water allocation during the optimization iteration process. Based on such time discretization, the trajectory position and water levels at any time node can be accurately extracted and called whenever necessary during the entire CMD optimization process. The dynamic continuity of the crane lifting and the ballast operation between different discrete time nodes are ensued by introducing necessary constraints of basic dynamics rules into the CMD optimization process. The cooperative matching relationship is determined by the one-to-one correspondences between the real-time trajectory position and the real-time ballast state with respect to specific time discrete point, namely each lifting trajectory position and the corresponding ballast state are associated through a unique time node. Such association between the trajectory position and the corresponding ballast state is established based on the relevant constraints of the operation safety requirements of RFC.

From the above analysis, pseudocodes of the solution process of the CMD method proposed in this study is explained in Table 1. From Table 1, the solution/calculation procedures of the proposed CMD method are detailedly as follows:

(i) Based on the working conditions and the engineering requirements of the offshore lifting operations, the design variables and the corresponding ranges are firstly determined for the CMD method;

(ii) The same as the general optimization processes, all the determined design variables should be initialized within the reasonable boundaries so as to start the CMD optimization processes;

(iii) A complete optimization loop is set at this step. The execution conditions of this loop are set to be the iteration residual of the objective function is greater than the residual standard value or the number of iterations is less than the maximum allowable iteration times;

(iv) While executing the optimization loop, intermediate models of the lifting trajectory and the ballast water allocation are constructed, ensuring that the lifting trajectory and water levels can be known at any iteration;

(v) Then, the entire operation time domain is discretized, and the one-to-one correspondences between the lifting trajectory positions and the water levels are established;

(vi) For this step, the CMD optimization goal is derived and the optimization iteration is executed to satisfy the given constraint conditions;

(vii) After the current optimization iteration is completed, the trajectory and water level design variables are updated and the next optimization loop is performed;

(viii) When the optimization iteration process satisfies the execution conditions, the optimization iteration continues. Conversely, when the optimization iteration process does not meet the execution conditions, the optimization iteration ends, and the optimal CMD scheme of lifting trajectory and ballast water allocation is obtained.

3. Optimization model establishment of the CMD method for RFC

3.1. Dynamics modeling for trajectory planning

To guarantee sufficient precision and reliability in the lifting trajectory planning, the establishment of an exact and trustworthy dynamics model of the lifting process is crucial (Zhang et al., 2010). Furthermore, this dynamics model serves as a critical foundation for realizing the CMD of the RFC lifting trajectory and ballast water allocation.

In this study, the Lagrangian method (Book, 1984) is utilized for the dynamics modeling of the lifting process of the RFC. In general, the working trajectory of a mechanical system is directly determined by the actions of its key structures. In this study, the lifting trajectory of an RFC is determined by the rotation of the base, the amplitude change of the boom, and the lifting movement of the hoist cable. Therefore, the crane system of RFC in this study is equivalent to a system with three degrees of freedom (Li et al., 2023b), encompassing the rotation of the base, the amplitude change of the boom, and the lifting movement of the hoist cable. A corresponding coordinate system is established for the crane: the origin point O_c is set at the intersection of the rotating axis of the base and the installation platform; the hull length, the hull width, and the vertical direction of the installation

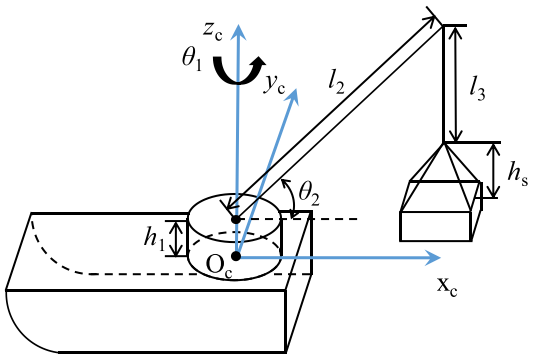

Fig. 5. Simplified diagram of the crane.

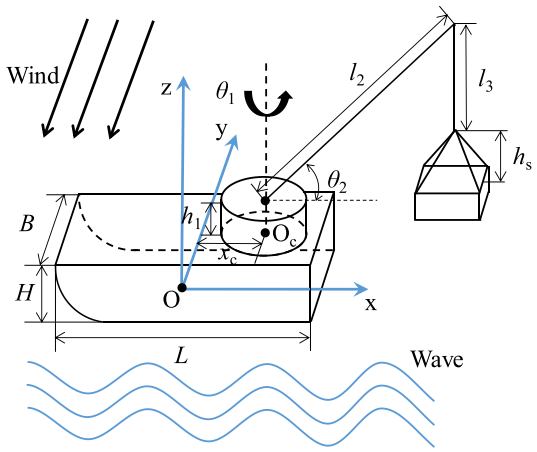

Fig. 6. The coordinate system establishment of lifting trajectory planning of the RFC.

platform are designated as the x_c axis, y_c axis, and z_c axis, respectively, as depicted in Fig. 5. In actual lifting operations, the lifting trajectory is determined by the combined effects of the rotation of the crane base, the amplitude change of the boom, and the lifting movement of the hoist cable. Therefore, the base rotation angle θ_1 (degree), the boom amplitude angle θ_2 (degree), and the length of the hoist cable l_3 (m) are set as the generalized coordinates. The corresponding Lagrangian dynamics equations are established as follows:

$$\begin{cases} \frac{d}{dt}\left(\frac{\partial E}{\partial \dot{\theta}_1}\right) - \frac{\partial E}{\partial \theta_1} + \frac{\partial V}{\partial \theta_1} = T_1 \\ \frac{d}{dt}\left(\frac{\partial E}{\partial \dot{\theta}_2}\right) - \frac{\partial E}{\partial \theta_2} + \frac{\partial V}{\partial \theta_2} = T_2 \\ \frac{d}{dt}\left(\frac{\partial E}{\partial \dot{l}_3}\right) - \frac{\partial E}{\partial l_3} + \frac{\partial V}{\partial l_3} = F_3 \end{cases} \tag{7}$$

where, T_1 (N·m) is the driving torque of the base, T_2 (N·m) is the driving torque of the boom, F_3 (N) is the lifting force of the hoist cable, E (kJ) is the total kinetic energy of the lifting system, and V (kJ) is the total potential energy of the lifting system.

The total kinetic energy E includes the kinetic energy of the crane base E_1 (kJ), the kinetic energy of the boom E_2 (kJ), and the kinetic energy of the crane load E_3 (kJ), expressed as follows:

$$\begin{aligned} E &= E_1 + E_2 + E_3 \\ &= \frac{1}{2} I_1 \dot{\theta}_1^2 + \frac{1}{2} I_2 \dot{\theta}_2^2 + \frac{1}{2} m_b v_2^2 + \frac{1}{2} m v^2 \end{aligned} \tag{8}$$

where, I_1 (kg·m^2) and I_2 (kg·m^2) represent the moment of inertias of the base and the boom, respectively; $\dot{\theta}_1$ (degree/s) and $\dot{\theta}_2$ (degree/s) represent the angular speeds of the base and the boom, respectively; v_2 (m/s) represents the linear velocities of the center of gravity of the boom, v (m/s) represents the linear velocities of the center of gravity of the crane load, m_b (t) is the mass of the boom, and m (t) is the mass of the crane load.

The total potential energy E_t (kJ) includes the potential energy of the base E_{t1} (kJ), the potential energy of the boom E_{t2} (kJ), and the potential energy of the crane load E_{t3} (kJ). Defining the plane where the crane base is located as the zero potential energy surface, the total potential energy E_t can be expressed as follows:

$$\begin{aligned} E_t &= E_{t1} + E_{t2} + E_{t3} \\ &= m_1 g h_{1c} + m_b g(h_1 + l_{2c} \sin\theta_2) + mg(h_1 + \cdots \\ &\quad l_2 \sin\theta_2 - l_3 - h_t - h_m) \end{aligned} \tag{9}$$

where, m_1 (t) represents the mass of the base, g (m/s^2) is the constant of gravitational acceleration (which is taken as 9.8 m/s^2 in this paper), h_{1c} (m) represents the height of the center of mass of the base, h_1 (m) is the height of the base, l_{2c} (m) represents the distance between the center of mass of the boom and the center of rotation of the boom, l_2 (m) is the length of the boom, h_s (m) is the distance between the hook and the upper surface of the crane load, and h_m (m) is the distance between the center of mass of the crane load and its upper surface. In conclusion, by substituting Eqs. (8) and (9) into Eq. (7), the complete Lagrange dynamics equation can be written as:

$$\begin{cases} T_1 = & \frac{1}{2} m_1 r_1^2 \ddot{\theta}_1 + m_b l_{2c}^2 \cos^2\theta_2 \ddot{\theta}_1 \\ & + m\ddot{\theta}_1 l_2^2 \cos\theta_2^2 \\ T_2 = & m_b l_{2c}^2 \ddot{\theta}_2 + \frac{1}{12} m_b l_2^2 \ddot{\theta}_2 + m\ddot{\theta}_2 l_2^2 - m\ddot{l}_3 l_2 \\ & \cos\theta_2 + m\dot{l}_3 l_2 \sin\theta_2 \dot{\theta}_2 + m_b l_{2c}^2 \dot{\theta}_1^{\,2} \\ & \sin\theta_2 \cos\theta_2 + m\dot{\theta}_1^{\,2} l_2^2 \sin\theta_2 \cos\theta_2 \\ & - 2 l_2 \dot{l}_3 \dot{\theta}_2 \sin\theta_2 + m_b g l_{2c} \cos\theta_2 \\ & + mg l_2 \cos\theta_2 \\ F_3 = & m l_2 \dot{\theta}_2^{\,2} \sin\theta_2 - m l_2 \ddot{\theta}_2 \cos\theta_2 \\ & + m\ddot{l}_3 - mg \end{cases} \tag{10}$$

where, r_1 (m) is the radius of the base; $\ddot{\theta}_1$ (degree/s^2) is the rotary angle acceleration; $\ddot{\theta}_2$ (degree/s^2) is the boom angle acceleration; and $\ddot{l}_3$ (m/s^2) is the lifting acceleration.

3.2. Design variables

For the entire process of intelligent RFC offshore lifting operations, the design variables of the CMD optimization model established in this section mainly come from two aspects: trajectory planning and ballast water allocation.

(1) Trajectory planning

The lifting trajectory of an RFC is typically defined as the curve swept by the center of gravity of the load in space. As it is a three-dimensional space curve, it can be decomposed into displacements in x, y, and z directions. To describe the position coordinates of the lifting trajectory at any time, the establishment of the corresponding spatial coordinate system is shown in Fig. 6. This coordinate system uses the intersection point of the base plane, the middle longitudinal section, and the middle cross-section as the coordinate origin O. Among them, the intersection line of the base plane and the middle longitudinal section is the x axis, heading towards the bow is positive, and towards the stern is negative. The intersection line of the base plane and the middle cross-section is the y axis, with the direction towards the left side being positive and towards the right side being negative. The intersection line of the middle cross-section and the middle longitudinal section is the z axis, with the direction upwards being positive and downwards negative. Therefore, the expressions of the displacement of the lifting trajectory in x, y, and z axes are as follows:

$$D_x = l_2 \cos\theta_2 \cos\theta_1 + x_r \tag{11}$$

$$D_y = l_2 \cos\theta_2 \sin\theta_1 \tag{12}$$

$$D_z = H + h_1 + l_2 \sin\theta_2 - l_3 - h_s - h_m \tag{13}$$

where, x_r (m) represents the longitudinal distance between the rotation center of the crane and the origin of the coordinate system, and H (m) denotes the moulded depth of the RFC.

According to Eqs. (11) to (13), the real-time position coordinates of the RFC lifting trajectory depend on the real-time crane rotation angle θ_1, the boom luffing angle θ_2, and the hoist cable length l_3. As explicated in Section 2.2, the PTP theory facilitates the transformation of an optimal control problem into a nonlinear constraint problem that requires solving corresponding polynomial coefficients.Thus, the selection of an appropriate polynomial degree is crucial for effectively defining variables. Wang et al. (2018) conducted an in-depth study on the impact of polynomial degree on the working trajectory planning, results suggesting that the sixth-degree polynomial trajectory can yield the optimal energy consumption and significantly reduce the solution time of the optimization program compared to other degrees. Consequently, this study also adopts a sixth-degree polynomial to depict the variations in θ_1, θ_2, and l_3:

$$\theta_1(t) = p_{10} + p_{11}t + p_{12}t^2 + p_{13}t^3 + p_{14}t^4 \cdots + p_{15}t^5 + p_{16}t^6 + \theta_{10} \tag{14}$$

$$\theta_2(t) = p_{20} + p_{21}t + p_{22}t^2 + p_{23}t^3 + p_{24}t^4 \cdots + p_{25}t^5 + p_{26}t^6 + \theta_{20} \tag{15}$$

$$l_3(t) = p_{30} + p_{31}t + p_{32}t^2 + p_{33}t^3 + p_{34}t^4 \cdots + p_{35}t^5 + p_{36}t^6 + l_{30} \tag{16}$$

where, p_{jk}'s are the polynomial coefficients; j denotes the identifiers for the crane base ($j = 1$), the boom ($j = 2$) and the hoist cable ($j = 3$); k is the serial number of the polynomial coefficient; θ_{10} (degree) is the initial rotation angle of the crane base; θ_{20} (degree) is the initial luffing angle of the boom; and l_{30} (m) is the initial length of the hoist cable.

Furthermore, solving the polynomial coefficients requires the introduction of relevant boundary conditions. At the initial and final instants, the crane rotation angle θ_1, the boom luffing angle θ_2, and the hoist cable length l_3 depend on the initial and final positions set by the actual offshore lifting task. In addition, due to high safety requirements during offshore lifting, the RFC should not experience rigid or flexible impacts during rotation, luffing, or lifting. Consequently, the initial and final states of offshore lifting operations (including speed and acceleration) should be restricted to 0. In summary, once the appropriate boundary conditions are established, all coefficients except p_{16}, p_{26}, and p_{36} can be determined through Eq. (6). Therefore, p_{16}, p_{26}, and p_{36} should be selected as design variables in the process of identifying the optimal lifting trajectory. Moreover, since the final time instant of the lifting operation, t_f (min), is not constant, it should also be considered as a design variable. Hence, during the trajectory planning process, the associated design variables $\boldsymbol{x_t}$ are identified as follows:

$$\boldsymbol{x_t} = [p_{16}, p_{26}, p_{36}, t_f] \tag{17}$$

where, the upper and lower boundaries for the polynomial coefficients p_{16}, p_{26}, and p_{36} are determined by the properties of the PTP method, typically ranging from negative infinity to positive infinity. The lower boundary of t_f is zero, while the upper boundary should be determined based on the conventional manual operation to ensure a sufficient amount of time for completing the intelligent lifting task. In this case study, the upper boundary of t_f is set to 30 min. The upper and lower boundaries of the design variables regarding the lifting trajectory planning are listed in Table 2.

(2) Ballast water allocation

In this section, it is assumed that the total number of ballast tanks used to maintain the stability of the RFC is denoted as q. For ballast tank p ($p = 1, 2, 3, \ldots, q$), based on the PTP theory, a 6th degree polynomial is employed to represent the changes in its water level:

$$\Delta h_p = |h_{pf} - h_{p0}| \, |w_{p0} + w_{p1}t + w_{p2}t^2 + w_{p3}t^3 + w_{p4}t^4 \cdots + w_{p5}t^5 + w_{p6}t^6| \tag{18}$$

where, w_{pk}'s are the polynomial coefficients, h_{p0} (m) represents the initial water level of ballast tank p, and h_{pf} (m) represents the final water level of ballast tank p. Similarly, while seeking the optimal ballast water allocation optimization scheme, w_{p6} and h_{pf} should be selected as design variables.

At the pre-ballast stage of the RFC, different situations of the initial allocation of the ballast water have notable different effects on the subsequent ballast performances. Thus, this study also optimizes the initial water level in each ballast water tank and the initial ballast water load for the pre-ballast stage. Consequently, the initial water level h_{p0} in each ballast tank is selected as a design variable in this study. Furthermore, to prevent the foreign objects existing in the external seawater from disrupting the real-time exchange of ballast water between the internal ballast tanks and the external seawater, the ballasting process in this study is determined to utilize the internal allocation mode. In addition, the initial quantity of the ballast water, Q_0 (t), should meet the normal operation requirements of subsequent tasks. While fulfilling the requirements for ship safety and stability, the initial quantity of the ballast water should be minimized as much as possible to prevent redundancy, which could undermine the ballasting efficiency. Excessive ballast water may prolong the water injection and drainage time before and after the RFC lifting operations, with limited enhancement to ship stability. Therefore, the initial ballast water load Q_0 is also selected as a design variable.

From the above analysis, the corresponding design variables $\boldsymbol{x_b}$ of the RFC ballast water allocation process are summarized as follows:

$$\boldsymbol{x_b} = [w_{p6}, h_{p0}, h_{pf}, Q_0] \tag{19}$$

Based on the characteristics of the PTP theory, the range of w_{p6} is set between negative infinity and positive infinity. In the process of ballast water allocation, the water levels in each ballast tank cannot exceed the structural height of the tank h_{max}. Moreover, the lower boundary of the initial ballast water load Q_0 is the minimum load Q_{min} required to maintain ship stability, and the upper boundary is the maximum load Q_{max} after all internal ballast tanks of the ship are filled. In summary, the upper and lower boundaries corresponding to the design variables of the ballast water allocation are listed in Table 3.

Table 2
Upper and lower boundaries of the design variables regarding the lifting trajectory planning.

Design variable (unit)	Lower bound	Upper bound
p_{16}	$-\infty$	$+\infty$
p_{26}	$-\infty$	$+\infty$
p_{36}	$-\infty$	$+\infty$
t_f (min)	0	30.00

Table 3
Upper and lower boundaries of the design variables regarding the ballast water allocation.

Design variable (unit)	Lower bound	Upper bound
w_{p6}	$-\infty$	$+\infty$
h_{p0} (m)	0	h_{max}
h_{pf} (m)	0	h_{max}
Q_0 (t)	Q_{min}	Q_{max}

3.3. Objective function

For the CMD of the lifting trajectory planning and the ballast water allocation, the main goal is to maximize the overall offshore operation

performance of the RFC. However, this is not a single-dimensional performance metric but encompasses multiple criteria. Thus, in this study, four key indicators of the RFC operation performances are considered from the perspectives of safety, environmental protection, and efficiency. These include the operation safety, the energy consumption of the crane, the energy consumption of the ballast system, and the time cost.

(1) Operation safety

The operation safety is the primary prerequisite in the offshore lifting process, mainly manifested in whether the heel and trim angles of the ship are within safe ranges. Typically, due to the structural characteristics of the RFC, the total length of the ship greatly exceeds its width, resulting in a much larger longitudinal stability moment than the transverse stability moment. Therefore, in the actual lifting process, the ship is more prone to severe roll, creating a safety hazard. Thus, the limit heel angle θ_{lim} (degree) is chosen to minimize as the optimization objective in this study for ensuring the operation safety. The corresponding expression is as follows:

$$\theta_{lim} = \max\left\{ \left| \arctan\left(\frac{m(D_y - D_{y0}) + m_2(y_{2g} - y_{2g0})}{(\Delta + m)\overline{G_1 M_1}} + \frac{Q_0(y_b - y_{b0}) + \boldsymbol{M}_{\boldsymbol{Ey}}}{(\Delta + m)\overline{G_1 M_1}} \right) \right| \right\} \tag{20}$$

where, D_{y0} (m) represents the initial lateral position of the load center of gravity, y_{2g} (m) represents the lateral position of the boom center of gravity during the lifting process, y_{2g0} (m) represents the initial lateral position of the boom center of gravity, $\boldsymbol{M}_{\boldsymbol{Ey}}$ (N·m) represents the lateral environmental moment experienced by RFC, Δ(t) represents the ship's displacement, $\overline{G_1 M_1}$ (m) represents the transverse stability height after the ship is loaded, y_b (m) represents the lateral position of the equivalent tank center of gravity, and y_{b0} (m) represents the initial lateral position of the equivalent tank center of gravity, i.e.,

$$y_b = \frac{\sum_{p=1}^{8} \rho_w h_P S_p y_p}{Q_0} \tag{21}$$

where, ρ_w (kg/m^3) represents the density of seawater, y_p (m) represents the lateral position of the tank p center of gravity, and S_p (m^2) represents the floor area of the tank p.

(2) Energy consumption of the crane

Since the loading mass of the RFC is usually large, the crane often consumes a large amount of energy during the lifting operation. As known, different lifting trajectories may formulate various lifting activities leading to corresponding differences in energy consumption. Therefore, carrying out the lifting operation while minimizing energy consumption has become a main optimization objective of the CMD optimization model established in this study. The energy consumption of the crane E_L (kJ) can be obtained by:

$$E_L = \Delta t \left[\sum_{\varepsilon=1}^{\lambda} M_1(t)\dot{\theta}_1(t) + \sum_{\varepsilon=1}^{\lambda} M_2(t)\dot{\theta}_2(t) + \sum_{\varepsilon=1}^{\lambda} F_3(t)\dot{l}_3(t) \right] \tag{22}$$

where, Δt (min) denotes the equal time interval of the lifting operation after discretization:

$$\Delta t = \frac{t_f - t_i}{\lambda} \tag{23}$$

where, λ represents the number of intervals in which the entire time domain is discretized, and t_i (min) represents the initial time instant of the lifting operation.

(3) Energy consumption of the ballast system

From the perspective of the ballast operation, the primary goal is to timely and accurately balance the amount of ballast water in each tank during the crane's rotation process, to maintain the stable balance of the hull. Furthermore, it is important to consider how to reduce energy consumption as much as possible while ensuring accurate ballasting, because only when the energy consumption of both the crane and the ballast system is reduced, the overall energy-saving performance of RFC in offshore lifting operations can be truly improved. Therefore, the energy consumption of the ballast system E_B (kJ) is one of the optimization objectives, and the expression is:

$$E_B = \rho_w g H_B \Delta t \sum_{\varepsilon=1}^{\lambda} \sum_{p=1}^{q} S_p \dot{h}_p(t)/\eta_B \tag{24}$$

where, H_B (m) represents the head of the ballast pump, $\dot{h}_p(t)$ (m/s) represents the change rate of water level in ballast tank p, and η_B represents the efficiency of the ballast pump.

(4) Time cost

Evaluating the efficiency of operations is a critical metric in many engineering projects and a high efficiency correlates to lower time costs. Consequently, this study aims to minimize time costs during operations while carefully considering the collaborative matching between the crane and ballast systems.

By setting these four objective functions, the offshore operation performance of the RFC can be significantly enhanced. In summary, the objective function can be written as:

$$\min \quad [\theta_{lim}, E_L, E_B, t_f] \tag{25}$$

Apparently, the CMD of RFC lifting trajectory and ballast water allocation presents a multi-objective optimization problem. Given this study is to devise an efficient and reliable optimization method for the intelligent offshore operations of the RFC, this multi-objective optimization problem is converted into a single-objective optimization problem by attributing expert-based weights to each objective. This transformation reduces the decision-making difficulty and enhances the computational efficiency. In practical operations, technical experts can adjust these weights based on the actual requirements of offshore operations, such as sea conditions, types of lifted goods, etc. Consequently, the objective function of the CMD model for RFC lifting trajectory and ballast water allocation developed in this study is transformed into:

$$\min \quad f = \theta_{lim}^{\gamma_1} \bullet E_L^{\gamma_2} \bullet E_B^{\gamma_3} \bullet t_f^{\gamma_4} \tag{26}$$

where, γ_1, γ_2, γ_3, and γ_4 correspond to the weights of the limit heel angle θ_{lim}, the energy consumption of the crane E_L, the energy consumption of the ballasting system E_B, and the time cost t_f, respectively ($0 \leqslant \gamma_1, \gamma_2, \gamma_3, \gamma_4 \leqslant 1$, $\gamma_1+\gamma_2+\gamma_3+\gamma_4 = 1$). Their respective values are adjusted based on the specific requirements of offshore operations.

3.4. Constraints

In the process of offshore lifting operations for the RFC, constraints and limitations from multiple perspectives such as operational safety, motion control, and extreme working conditions should be implemented. It is essential to achieve safe, energy-saving, and efficient collaborative matching between the lifting trajectory and ballast water allocation.

(1) Hull inclination constraints

At the beginning of the lifting task, the heel and trim angles of the RFC should be maintained at 0°, i.e., $\theta_i = 0°$, $\phi_i = 0°$. While RFC operating, the safe range for the heel angle θ is −5° to +5°, and the safe range for the trim angle ϕ is −2° to +2° (CCS, 2016), namely

$$-5° \leqslant \theta \leqslant +5° \tag{27}$$

$$-2° \leqslant \phi \leqslant +2° \tag{28}$$

(2) Water level constraint of ballast tanks

During the internal allocation process of the ballast system, the maximum water level in each ballast tank cannot exceed the corresponding structural tank height:

$$0 \leqslant h_p \leqslant T_{pH} \tag{29}$$

where, T_{pH} (m) is the height of ballast tank p.

(3) The flow rate constraint of the ballast water allocation

The ballast water allocation process between different tanks is determined by the suction and drainage actions of the ballast pump. Therefore, the total flow rate of the ballast water allocation Q_f (t/min) during the lifting operation cannot exceed the maximum flow rate Q_L (t/min) that the ballast pump can provide, i.e.,

$$Q_f \leqslant Q_L \tag{30}$$

(4) Boom amplitude angle constraint

The amplitude angle of the boom determines the outboard distance of the loading mass, which should neither be too large nor too small during actual lifting operations. An excessively large outboard distance increases the overturning moment caused by the load, which either exacerbates the load on the ballasting system or risks destabilizing the hull. Conversely, a too small outboard distance reduces the load on the ballasting system, but may cause interference between the load and the hull structure or the crane itself. Therefore, the amplitude range of the boom during actual lifting operations should be determined based on the characteristics of the RFC:

$$\theta_{2min} \leqslant \theta_2 \leqslant \theta_{2max} \tag{31}$$

where, θ_{2min} (degree) represents the minimum threshold for the allowable boom amplitude angle, and θ_{2max} (degree) represents the maximum threshold for the allowable boom amplitude angle.

(5) The length variation constraint of the hoist cable

The vertical position variation of the crane load is mainly determined by the rise and fall of the hoist cable, wherein the length variation interval of the hoist cable is:

$$l_{3min} \leqslant l_3 \leqslant l_{3max} \tag{32}$$

where, l_{3min} (m) represents the minimum extension length of the hoist cable, and l_{3max} (m) represents the maximum extension length of the hoist cable.

(6) Speed and acceleration constraints of lifting activities

While the crane executing the rotating, luffing, and hoisting activities, it is necessary to consider the maximum speed and acceleration of the crane system to meet the basic dynamics requirements, namely

$$\dot{\theta}_1 \leqslant \dot{\theta}_{1max}, \quad \ddot{\theta}_1 \leqslant \ddot{\theta}_{1max} \tag{33}$$

$$\dot{\theta}_2 \leqslant \dot{\theta}_{2max}, \quad \ddot{\theta}_2 \leqslant \ddot{\theta}_{2max} \tag{34}$$

$$\dot{l}_3 \leqslant \dot{l}_{3max}, \quad \ddot{l}_3 \leqslant \ddot{l}_{3max} \tag{35}$$

where, $\dot{\theta}_1$ (degree/s), $\dot{\theta}_2$ (degree/s), and $\dot{l}_3$ (m/s) represent the speed thresholds of crane rotation, amplitude change, and lifting motion, respectively; and $\ddot{\theta}_1$ (degree/s^2), $\ddot{\theta}_2$ (degree/s^2), and $\ddot{l}_3$ (m/s^2) denote the acceleration thresholds of crane rotation, amplitude change, and lifting motion under safe and stable lifting operations, respectively.

(7) Power constraints

The maximum instantaneous power consumed by the driving device during crane rotation, amplitude change, and lifting motion cannot exceed the rated power of the corresponding driving elements can provide, i.e.,

$$P_{1max} \leqslant P_{1e} \tag{36}$$

$$P_{2max} \leqslant P_{2e} \tag{37}$$

$$P_{3max} \leqslant P_{3e} \tag{38}$$

where, P_{1max} (kW), P_{2max} (kW), and P_{3max} (kW) represent the instantaneous power consumed by the driving device during crane rotation, amplitude change, and lifting motion, respectively; and P_{1e} (kW), P_{2e} (kW), and P_{3e} (kW) represent the rated power of the driving device during crane rotation, amplitude change, and lifting motion, respectively.

(8) Target lifting position constraints

In order to ensure the accuracy of the RFC lifting trajectory planning, the ending position of the lifting trajectory must be consistent with the preset target lifting position, that is:

$$D_{xf} = l_2 \cos\theta_{2f} \cos\theta_{1f} + x_c \tag{39}$$

$$D_{yf} = l_2 \cos\theta_{2f} \sin\theta_{1f} \tag{40}$$

$$D_{zf} = H + h_1 + l_2 \sin\theta_{2f} - l_{3f} - h_s - h_m \tag{41}$$

where, D_{xf} (m), D_{yf} (m), and D_{zf} (m) represent the displacement of the target lifting position decomposed in x, y, and z directions, respectively.

(9) Ballast water quantity constraint

Throughout the entire ballasting process, the total amount of ballast water loaded by the RFC should remain constant and equal to the initial ballast water quantity Q_0, which can be written as:

$$Q(t) = \sum_{p=1}^{q} \rho_w g S_p h_p(t) = Q_0 \tag{42}$$

where, $Q(t)$ (t) represents the total amount of ballast water loaded in each tank at time t.

In summary, all the inequality constraints $\boldsymbol{g}$ and equality constraints $\boldsymbol{h}$ in the CMD optimization model for RFC lifting trajectory planning and ballast water allocation are organized as follows:

$$\boldsymbol{g} = \begin{cases} g_1 : \theta - 5 \\ g_2 : -5 - \theta \\ g_3 : \phi - 2 \\ g_4 : -2 - \phi \\ g_5 : h_p - T_{pH} \\ g_6 : Q_f - Q_L \\ g_7 : \theta_2 - \theta_{2max} \\ g_8 : \theta_{2min} - \theta_2 \\ g_9 : l_3 - l_{3max} \\ g_{10} : l_{3min} - l_3 \\ g_{11} : \dot{\theta}_1 - \dot{\theta}_{1max} \\ g_{12} : \dot{\theta}_2 - \dot{\theta}_{2max} \\ g_{13} : \dot{l}_3 - \dot{l}_{3max} \\ g_{14} : \ddot{\theta}_1 - \ddot{\theta}_{1max} \\ g_{15} : \ddot{\theta}_2 - \ddot{\theta}_{2max} \\ g_{16} : \ddot{l}_3 - \ddot{l}_{3max} \\ g_{17} : P_{1max} - P_{1e} \\ g_{18} : P_{2max} - P_{2e} \\ g_{19} : P_{3max} - P_{3e} \end{cases} \tag{43}$$

$$\boldsymbol{h} = \begin{cases} h_1 : \quad l_2 \cos\theta_{2f} \cos\theta_{1f} + x_c - D_{xf} \\ h_2 : \quad l_2 \cos\theta_{2f} \sin\theta_{1f} - D_{yf} \\ h_3 : \quad H + h_1 + l_2 \sin\theta_{2f} - l_{3f} - h_s - h_m - D_{zf} \\ h_4 : \quad \theta_i \\ h_5 : \quad \phi_i \\ h_6 : \quad Q - Q_0 \end{cases} \tag{44}$$

3.5. Optimization model

By integrating the design variables, objective function, and constraints analyzed in Sections 3.2 to 3.4, the CMD model of the lifting trajectory planning and the ballast water allocation for the intelligent RFC can be established as below:

$$\begin{cases} \text{find} & \boldsymbol{x} = [\boldsymbol{x_t}, \boldsymbol{x_b}] \\ \text{min} & f = \theta_{lim}^{\gamma_1} \bullet E_L^{\gamma_2} \bullet E_B^{\gamma_3} \bullet t_f^{\gamma_4} \\ \text{s.t.} & \boldsymbol{g} = [g_1, g_2, \ldots, g_{19}]^T \leqslant \boldsymbol{0} \\ & \boldsymbol{h} = [h_1, h_2, \ldots, h_6]^T = \boldsymbol{0} \end{cases} \tag{45}$$

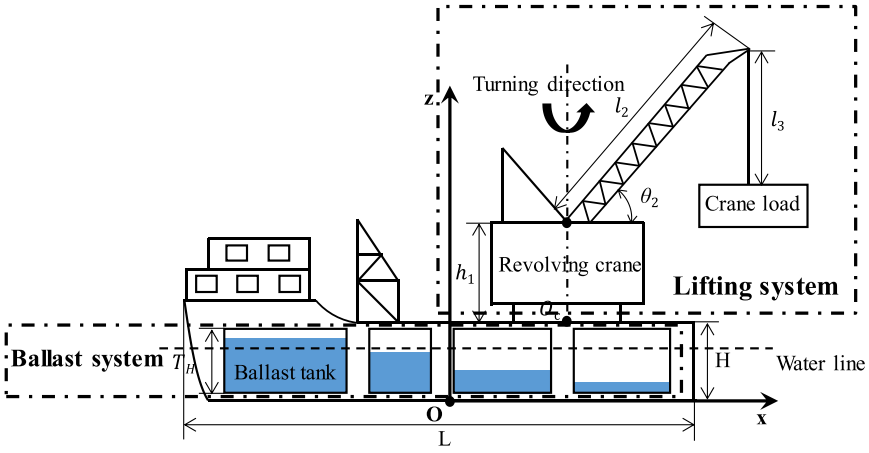

Fig. 7. Simplified diagram of the Minami Tenryu floating crane.

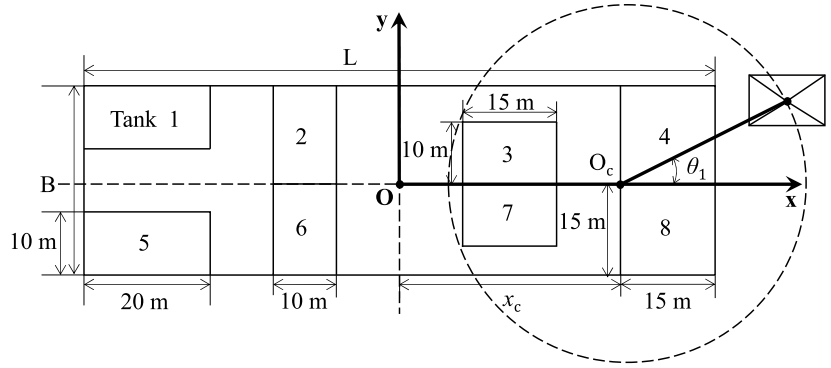

Fig. 8. Dimensions and layout of the ballast tanks of the RFC.

Table 4
Sea conditions during the lifting activities.

Parameter (unit)	Value
Wave scale	3.00
Wave direction (degree)	90.00
Wind speed (m/s)	10.30
Wind direction (degree)	80.00

Table 5
Key structure and performance parameters of RFC Minami Tenryu.

Parameter (unit)	Value	Parameter (unit)	Value
L (m)	100.00	x_c (m)	35.00
B (m)	30.00	T_H (m)	4.00
H (m)	8.00	H_B (m)	6.00
m_1 (t)	1571.46	l_2 (m)	75.00
m_2 (t)	314.29	P_{1e} (kW)	300.00
h_1 (m)	32.00	P_{2e} (kW)	400.00
r_1 (m)	11.64	P_{3e} (kW)	200.00
L_c (t)	450.00	Q_L (t/h)	3000.00
θ_{2min} (degree)	28.00	η_B	0.85
θ_{2max} (degree)	78.10		

4. Solution and analysis of the CMD for RFC

4.1. Case study of the CMD method for RFC

4.1.1. Parameter determination of the case study

In this section, the feasibility of the proposed CMD method is proved through a specific real-world case study. The RFC "Minami Tenryu" is selected as the research object and is set to lift a 300 t load. The starting position is (31.7, 0, 60.0) with a base rotation angle of 0° and a boom angle of 65°. The target position is (0, 19.4, 66.0) with a base rotation angle of 90° and a boom angle of 75°. The relevant parameters of sea conditions are detailed in Table 4. Notably, to simplify the solving process, this case disregards the energy loss caused by the flow of ballast water in the pipelines and adopts an internal allocation method for ballasting.

The simplified diagram of the Minami Tenryu is illustrated in Fig. 7, which mainly consists of an upper crane and an internal ballast system. Specifically, the crane includes a base that can perform rotational movement, a variable amplitude boom that can control the span, and a hoist cable responsible for lifting operations. The ballast system has 8 ballast tanks, and the ballast water is allocated between different tanks by the ballast pump. The dimensions and layout of the tanks are shown in Fig. 8, and the one-line diagram of the ballast system of the RFC is shown in Fig. 9. Table 5 lists the key structure and performance parameters of the Minami Tenryu, where L (m) is the length of the ship, B (m) is the breadth of the ship, and L_c (t) represents the rotary lifting capacity.

4.1.2. Result analysis of the case study

In this section, based on the specific requirements of offshore operations, weights of the objective function γ_1, γ_2, γ_3, and γ_4 are set to 0.4, 0.2, 0.2, and 0.2, respectively. The heuristic optimization method of genetic algorithm is adopted to solve the CMD problem, with the population size being 100, the iteration count being 50, the crossover rate being 0.8, and the mutation rate being 0.01. The computational environment comprises a Windows 10 operating system, a 2.60 GHz Intel (R) Core (TM) i7-10750H processor, and 8.0 GB of Random Access Memory (RAM).

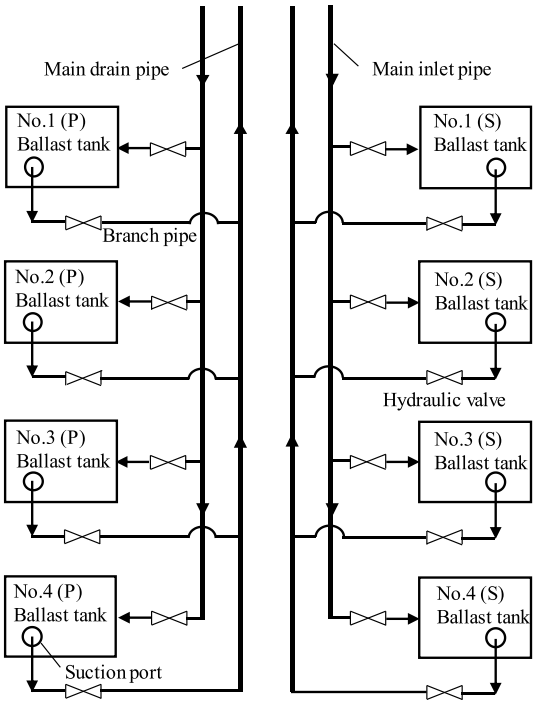

Fig. 9. The one-line diagram of the RFC ballast system.

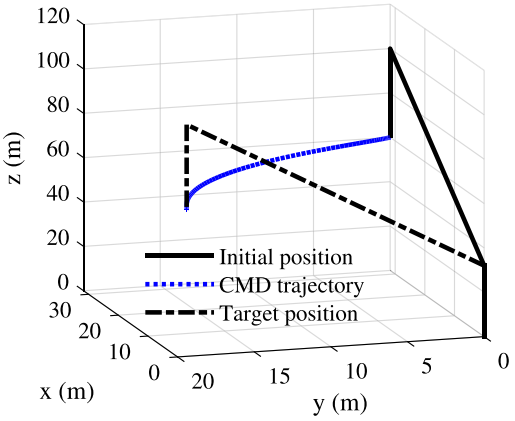

Fig. 10. The optimal lifting trajectory and the corresponding crane posture obtained by the CMD method.

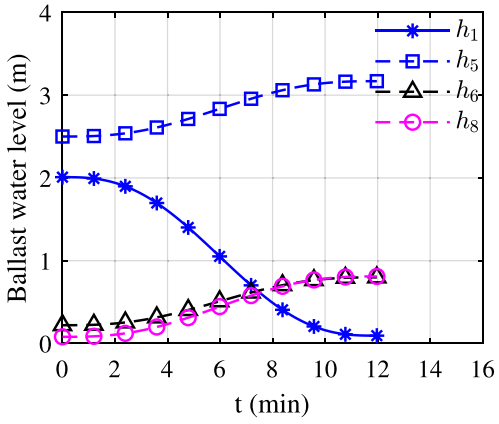

Fig. 11. The optimal ballast water level curves obtained by the CMD method.

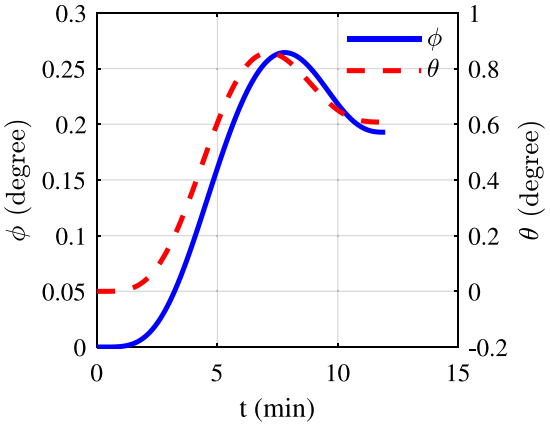

Fig. 12. The curves of the hull inclination angle obtained by the CMD method.

By solving the established CMD optimization model, the optimal lifting trajectory is obtained as illustrated in Fig. 10. It reveals that the optimal lifting trajectory obtained from the CMD method exhibits smooth, continuous, and non-sudden change characteristics overall, ensuring the stability of the RFC lifting operation. Therefore, it is evident that the proposed CMD method is capable of finding and determining the optimal trajectory according to specific lifting task requirements. As shown in Fig. 11, the water level changes in each ballast tank indicate that the optimal ballasting scheme involves four tanks participating in ballast water allocation. As the lifting operation progresses, the water level in Tank 1 gradually decreases until it is completely drained. In contrast, the water levels in Tanks 5, 6, and 8 show upward trends. By observing the water level change curves of all tanks, it can be seen that the curves are smooth and continuous without sudden changes, which positively contributes to ensuring the stability of the ballast operations. Fig. 12 depicts the curves of the hull inclination angle during the operation process. The heel angle is consistently maintained within 1°, and the trim angle change is minimal with the maximum value only reaching 0.27°, meeting the offshore operation safety requirements. From such operation safety and stability, it is evident that the CMD method successfully formulates an optimal collaborative matching operation scheme for RFC lifting trajectory and ballast water allocation, fully proving the feasibility of the method.

4.2. Superiority analysis of the CMD method

The conventional SD methods for RFC offshore lifting operations typically follow a strategy of “determining the optimal trajectory first, then determining the optimal ballast scheme”. Although such SD method can find the optimal ballast water allocation scheme under the given optimal trajectory, it fails to find the globally optimal lifting scheme for the entire operation process. Because the SD method does not take into account the coupling effects between the trajectory planning and ballast water allocation. To address this issue, the CMD method proposed in this study can compensate for deficiencies of the SD method.

In Section 4.1, a specific case study has been successfully solved using the CMD method, and corresponding results have been analyzed. To better understand the differences and relative superiority of the CMD and SD methods in practical applications, comparative analysis is performed in this section using the same case study as adopted in Section 4.1. By maintaining the same constraint conditions and objective functions with the CMD model, the optimal lifting trajectory obtained by the SD method is illustrated in Fig. 13. Clearly, under identical initial and final lifting positions, both the SD and CMD methods devise

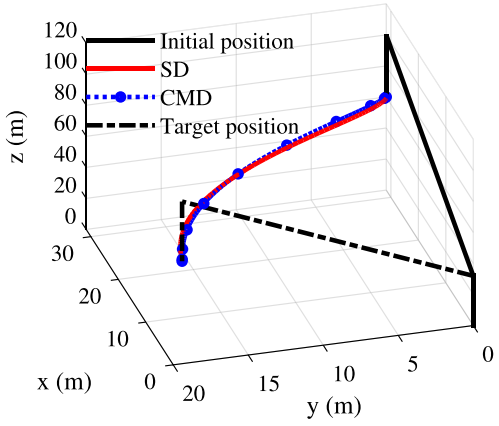

Fig. 13. The optimal lifting trajectories obtained by the SD method and the CMD method.

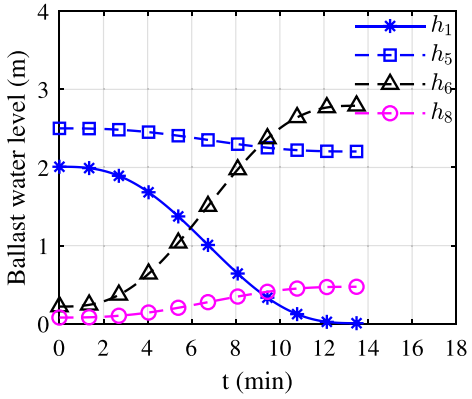

Fig. 14. The optimal ballast water level curves obtained by the conventional SD method.

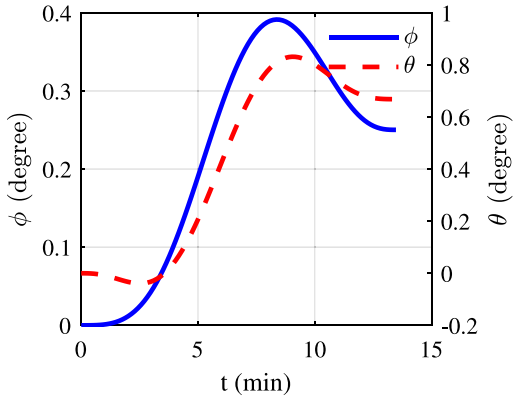

Fig. 15. The curves of the hull inclination angle obtained by the conventional SD method.

optimal lifting trajectories that maintain similar forms and exhibit smooth, continuous characteristics without abrupt changes.

Fig. 14 presents the curves of the optimal ballast water levels at each ballast tank determined by the SD method. By comparing with Fig. 11, certain similarities can be observed in the optimal ballasting schemes obtained from both methods. For example, both primarily involve four identical tanks (Tanks 1, 5, 6, 8) to accomplish the ballasting operations. As the crane rotates, the water level in ballast tank 1, situated on the same side as the load, gradually descends, while the water levels

Table 6
Comparison between the CMD and the SD methods.

Method	SD	CMD	Improvement
Lifting operation time (min)	13.48	11.97	−11.20%
Total energy consumption (10^4 kJ)	5.88	4.91	−16.50%
Ballast water allocation quantity (t)	486.75	399.92	−17.84%
Decision-making time (min)	6.77	3.08	−54.50%

in Tanks 6 and 8, on the opposite side of the load, display ascending trends. Nevertheless, the water level in tank 5 shows different situations regarding these two methods, namely an increasing trend in SD method and a decreasing trend in CMD method. By careful observation, in terms of the extent of water level variation in each ballast tank, the ballast scheme achieved by the SD method exhibits considerably higher fluctuations than the CMD method, particularly the water level changes in Tank 6.

The curves of the inclination angle achieved by the conventional SD method during the lifting operation are illustrated in Fig. 15. By comparing with the inclination angle obtained through the CMD method (as illustrated in Fig. 12), it is seen that both methods maintain the heel angle within 1.00° and the trim angle within 0.50°. This clearly demonstrates that both methods meet the safety standards for offshore lifting operations. However, a closer inspection reveals that the CMD method, compared to the SD method, yields a smaller range of heel angle variations (the heel angle obtained from CMD: 0°~0.86°; and the heel angle obtained from SD: −0.04°~0.83°) and effectively reduces the maximum trim angle by 32.46% (the maximum trim angle obtained from CMD: 0.39°; and the maximum trim angle obtained from SD: 0.26°). It implies that the CMD method can better ensure the safety and stability of the hull throughout the lifting operation.

Further, comprehensive comparisons and analysis between these two methods in aspects such as lifting operation time, total energy consumption, ballast water allocation amount, and decision-making time, are also carried out as listed in Table 6:

(1) Comparison of the lifting operation time

As shown in Table 6, the CMD method proposed in this study greatly shortens the lifting operation time compared with the SD method by 11.20% from 13.48 min to 11.97 min, namely improving the efficiency of the lifting operation significantly. The fundamental reason is that the ballast scheme formulated by the CMD method has a lower amount of ballast water allocation, which effectively shortens the ballasting operation time.

(2) Comparison of the total energy consumption

Table 6 compares the total energy consumption of lifting operations regarding the SD and CMD methods. Results reveal that the CMD method reduces the total energy consumption by 16.50%, substantially enhancing the energy efficiency. Upon detailed scrutiny, although the lifting energy consumption of the SD method (4.51×10^4 kJ) is marginally lower than that of the CMD method (4.91×10^4 kJ), the ballasting energy consumption of the SD method (7.16×10^4 kJ) significantly exceeds that of the CMD method (5.88×10^4 kJ). This phenomenon underscores the drawbacks of the SD method: although the SD method identifies a more energy-efficient lifting trajectory, it overlooks the impact of coupling effects between the lifting trajectory and the ballasting process. As a result, the total energy consumption escalates despite the reduction in lifting energy consumption due to the significant increase in ballasting energy consumption.

(3) Comparison of the ballast water allocation amount

According to Table 6, the proposed CMD method merely requires the allocation of 399.92 tons of ballast water throughout the entire operation, representing a reduction of 86.83 tons in comparison to the SD method. Essentially, the decrease in ballast water allocation also indirectly curtails the energy consumption of ballasting. The disparity is attributed to the consideration of the closely coupling relationships between the trajectory planning and the ballast water allocation. The

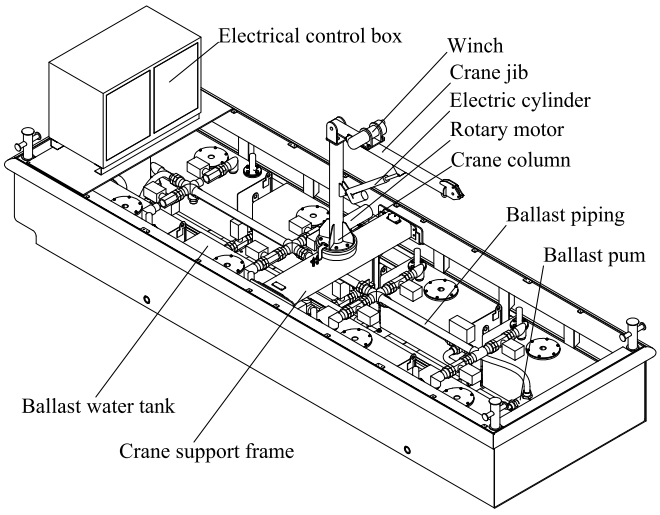

Fig. 16. The schematic diagram of the RFC test stand.

CMD method not only pursues the minimum energy consumption trajectory, but also balances the ballast water allocation process, to derive a globally optimal operation scheme.

(4) Comparison of the decision-making time

Observing Table 6, the CMD method displays a distinct advantage in decision-making time, saving more than half the time compared to the SD method. Indeed, this trend can be foreseen when the principle of SD method is introduced. Essentially, the SD method is a "two-step" optimization process, carrying out two separate optimizations for the trajectory planning and the ballast water allocation, respectively. Nevertheless, the CMD method integrates the lifting trajectory planning and ballast water allocation, leading to an "one-step" optimization calculation, causing a "cliff-like" drop in decision-making time. This shortened decision-making time better suits the quick and efficient response demands of the intelligent upgrade for the RFC.

Based on the analyses above, it can be concluded that the CMD method has apparent advantages compared with the SD method in terms of the lifting operation time, the total energy consumption, the ballast water allocation amount, and the decision-making time. Overall, the CMD method demonstrates superior performance over the SD method in actual offshore lifting operations.

5. Numerical and experimental validation of the CMD method

This section relies on the existing RFC test stand in the laboratory to perform the numerical and experimental validation for the efficacy of the CMD method proposed in this study. In actual offshore lifting operations, diverse lifting tasks are fundamentally the combinations of different lifting trajectories and loading masses. Therefore, these two aspects regarding different lifting trajectories and loading masses should be the key elements of validation. For the optimization objective of the CMD method performed in this section, it is also to find the optimal lifting plan of the RFC to realize the maximum safety, the minimum energy consumption, and the highest working efficiency. Consequently, the corresponding optimization objective is aligned with Eq. (45), and the weight values of the objective function remain consistent as set in Section 4.1.2, namely $\gamma_1 = 0.4$, $\gamma_2 = 0.2$, $\gamma_3 = 0.2$, and $\gamma_4 = 0.2$, respectively.

5.1. RFC test stand establishment

The schematic diagram of the RFC test stand is presented in Fig. 16, in which the corresponding key structures and components are detailly noted, including the electrical control box, the winch, the crane jib, the ballast pipe system, the ballast pump, the ballast tanks, the electronic control valve, etc. The configuration of the ballast system is particularly critical to determine the quality of the physical experiment of the ballast water allocation. In order to facilitate the numerical analysis and system control, the ballast tanks of the RFC test stand are arranged symmetrically, as shown in Fig. 17, in which all ballast tanks are connected through pipelines. The ballast system of the test stand relies

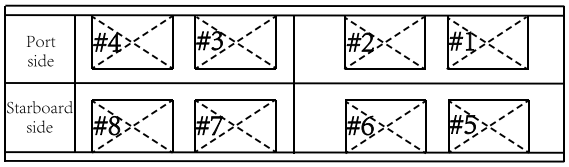

(a) Top view

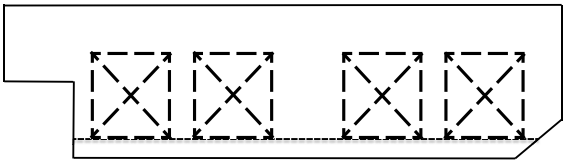

(b) Side view

Fig. 17. Layout of ballast tanks of the RFC test stand.

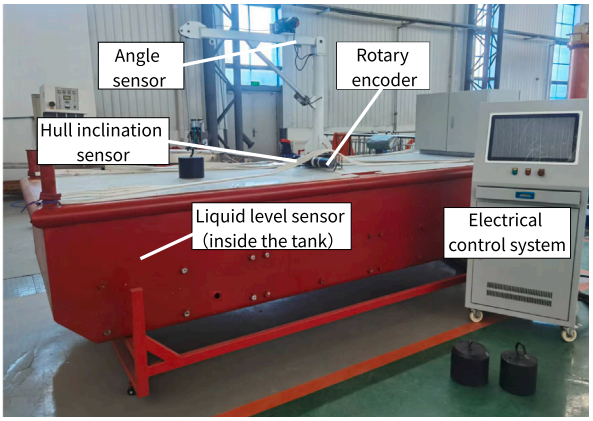

Fig. 18. The real physical structure of the RFC test stand.

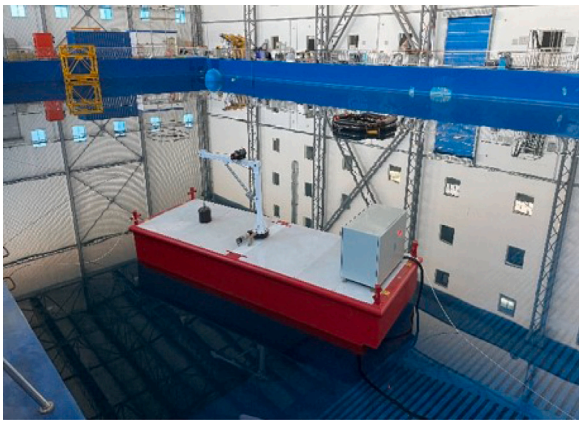

Fig. 19. The execution of lifting experiments of the RFC.

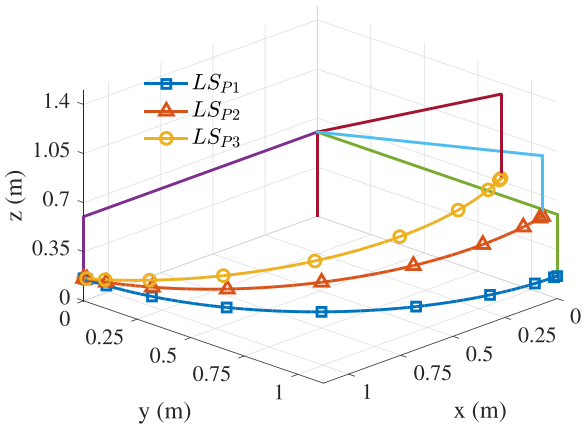

Fig. 20. The optimal lifting trajectories regarding different target positions obtained from the CMD method.

Table 7
Key parameters of the physical test stand of the RFC.

Parameter	Value/unit
Total length	4.50 m
Breadth	1.50 m
Depth	0.70 m
Empty ship mass	0.80 t
Ballast tank size	0.80 m × 0.30 m × 0.40 m
Number of ballast tanks	8
Ballast pump flow rate	2.00 m^3/h
Boom length	1.12 m
Amplitude range	0°~60.00°
Lifting capacity	0.05 t

on the intake pump and the drainage pump to complete the water supply and drainage operations. Each ballast tank is equipped with solenoid valves in the inlet and outlet pipes, respectively, to control the water supply and drainage actions, as illustrated in Fig. 16. The main parameters of this test stand are listed in Table 7.

The real physical structure of the RFC test stand is presented in Fig. 18. In order to realize the real-time data acquisition from the ballasting experiments of the RFC test stand, relevant sensors are installed at key positions, as illustrated in Fig. 18. A hull inclination sensor (two-axis obliquity sensor) is installed on the centerline of the hull to obtain real-time inclination data. An angle sensor is installed on the crane to measure the elevation angle of the jib. A rotary encoder installed on the slewing base of the crane is to measure the column slewing angle in real time. Each ballast tank is equipped with a liquid level sensor for real-time acquisition of the water level data of the corresponding tank. Additionally, the test stand is equipped with a complete electrical control system, which can collect real-time data from various sensors and display relevant results on the user interface. Crucially, the electrical control system can also automatically execute lifting operations according to manually input ballast and lifting control parameters obtained from the theoretical calculation.

The experiments are carried out in a laboratory pool with the dimensions being 50 m × 30 m × 5 m (length × width × height), providing superior conditions to ensure the successful completion of the experiment. For such a large weight and volume, it is necessary to use a gantry crane to pre-place the test stand into the laboratory pool. During this process, relatively large ripples may be caused sometimes in the laboratory pool. If the experiment is conducted immediately at this time, the ripples will lead to significant errors in the measurement of the ship's inclination by the inclination sensor. Hence, it is required to let the test stand still for 10 min to eliminate the influence of ripples on the experimental accuracy. During the experiment, the test stand can work smoothly being controlled by the obtained optimal controls and almost no ripples are generated in the laboratory pool, as shown in Fig. 19, thus the ripples will not have substantial impacts on the experimental accuracy.

While conducting the experiment, the optimal matching operation scheme (including the optimal lifting trajectory and optimal ballast water allocation plan) is first obtained by the proposed CMD method based on the specific working conditions. In the meanwhile, the corresponding logical instructions of the lifting activities and the ballasting actions are respectively written based on the optimal operation scheme. Then, the RFC test stand is controlled to perform the offshore lifting operations according to the logical instructions, as shown in Fig. 19. During the test process, the key experimental data, including the heeling angle, the trim angle and the time consumption are collected and recorded in real time for subsequent analysis.

5.2. Efficacy validation regarding different target positions

The lifting trajectory depends on the requirements of the lifting task. For comparative analysis and comprehensive experiment, the starting point of the lifting activities of the RFC test stand is set as the center of loading mass when the horizontal rotation angle and the amplitude angle of the boom are both 0°. Three ending positions with different amplitude angles relative to the horizontal plane are selected, namely 0°, 20°, and 40°, respectively. The horizontal rotation angles for these lifting activities are uniformly set to 90°, because the worst safety and stability occur when the load is at the 90° lifting position relative to the hull length. If the CMD method can formulate a safe and stable operating scheme at this position, it can successfully deal with other target positions as well. In this way, three different lifting scenarios with different trajectories are formed, and the starting and ending positions are listed in Table 8. In this numerical and experimental validation, the lifting load is uniformly set to 30 kg.

5.2.1. Numerical validation regarding different target positions

By adopting the proposed CMD method, the optimal matching schemes of the lifting trajectory and ballast water allocation can be obtained regarding these three lifting scenarios. The optimal lifting trajectories with respect to different target positions can be obtained as illustrated in Fig. 20. As seen, the lifting trajectories with respect to different target positions are continuous and smooth without abrupt changes, which conforms to the practical crane controls. The corresponding key control parameters of the optimal trajectories are illustrated in Fig. 21, from which it is obvious that the rotation speed of the crane base, the luffing speed of the lifting arm and the lifting speed of the rope are all smooth and satisfy the constraints. Thus, it can be concluded that the proposed CMD method can find the optimal lifting trajectory between arbitrary initial and target lifting positions.

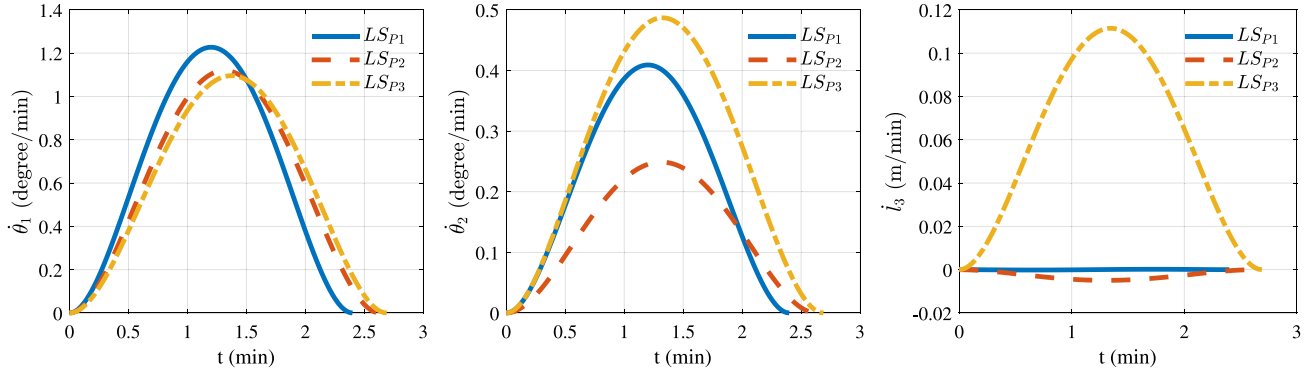

(a) The rotation speed of the crane base (b) The rotation speed of the lifting arm (c) The rotation speed of the rope

Fig. 21. The optimal control parameters obtained from the CMD method regarding different target positions.

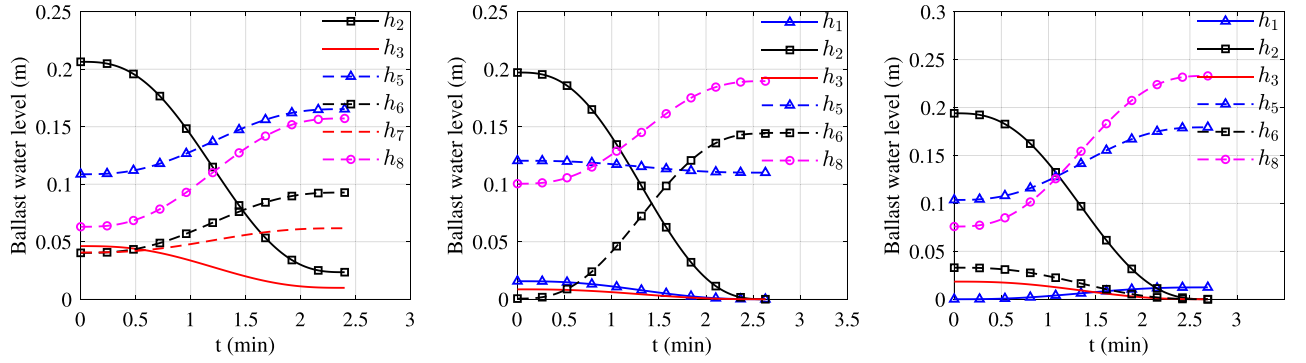

(a) The optimal ballast scheme regarding LS_{P1} (b) The optimal ballast scheme regarding LS_{P2} (c) The optimal ballast scheme regarding LS_{P3}

Fig. 22. The optimal ballast schemes obtained from the CMD method regarding different target positions.

Table 8
Operating scenarios regarding different target positions.

Lifting scenario	Starting position (Rotation angle, Amplitude angle)	Ending position (Rotation angle, Amplitude angle)
LS_{p1}	(0°, 0°)	(90.00°, 0°)
LS_{p2}	(0°, 0°)	(90.00°, 20.00°)
LS_{p3}	(0°, 0°)	(90.00°, 40.00°)

Fig. 22 depicts the optimal ballast schemes obtained from the CMD method regarding different target positions. Similarly, the control curves of the ballast water levels in all the tanks are continuous and smooth without abrupt changes, also conforming to the practical controls. As observed, the initial ballast water distributions of the RFC test stand regarding these three target positions are different, which is caused by the optimization process of the proposed CMD method. The optimal ballast scheme regarding target position LS_{P1} is illustrated in Fig. 22(a). It is seen that Tanks 1 and 4 do not involve in the ballast operations while undertaking LS_{P1} task. The water levels in Tanks 2 and 3 on the port side show decreasing trends in varying degrees, while the water levels in Tanks 5, 6, 7, and 8 on the starboard side show upward trends. For target position LS_{P2} as illustrated in Fig. 22(b), Tanks 4 and 7 do not participate in the ballast operations. The water levels in Tanks 2 and 5 on the port side show decreasing trends, while the water levels in Tanks 6 and 8 on the starboard side show upward trends in varying degrees. It is noticeable that the water level changes in Tanks 1 and 3 are very small relative to other tanks. Fig. 22(c) presents optimal ballast scheme regarding target position LS_{P3} and it can be observed that Tanks 4 and 7 do not involve in the ballast operations as well. The water levels in Tank 2 on the port side and Tank 6 on the starboard side show decreasing trends, while the water levels in Tanks 5 and 8 on the starboard side show upward trends. Nevertheless, the water levels in Tanks 1 and 3 change very little comparatively. The duration curves of the heel and trim angles of the RFC test stand are illustrated from Figs. 23 to 25 (the thick solid lines marked with "Theory"). It is indicated that both the heel and trim angles of the RFC test stand remain within the safe range throughout the lifting process (the safe range of heeling angle is −5°∼+5°, and the safe range of trim angle is −2°∼+2°), fully complying with the safety regulations.

Table 9
CMD results comparisons of the RFC test stand regarding different target positions.

Lifting scenario	LS_{P1}	LS_{P2}	LS_{P3}
Lifting operation time (min)	2.40	2.63	2.69
Total energy consumption (kJ)	20.21	21.16	22.45
Ballast water allocation quantity (kg)	54.39	57.08	60.17
Decision-making time (min)	0.43	0.42	0.43

Summarily, Table 9 lists the final results of the working performances obtained from the CMD method regarding different target positions. As seen, all of the lifting operation time, the quantity of the ballast water allocation, and the total energy consumption present upward trends with the vertical height of the trajectory ending point increasing. The decision-making time is almost the same regarding

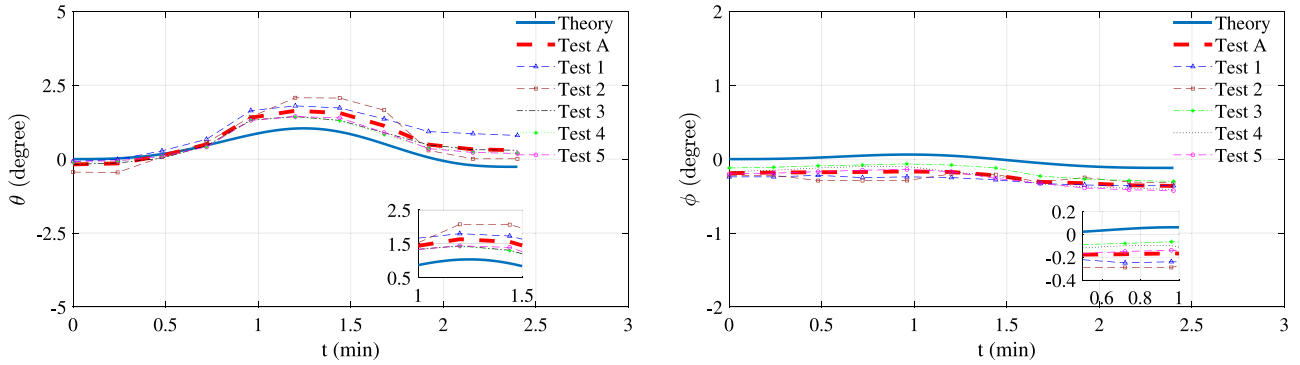

(a) The heel angle comparison (b) The trim angle comparison

Fig. 23. Comparison of theoretical and experimental inclination angles for lifting task LS_{P1}.

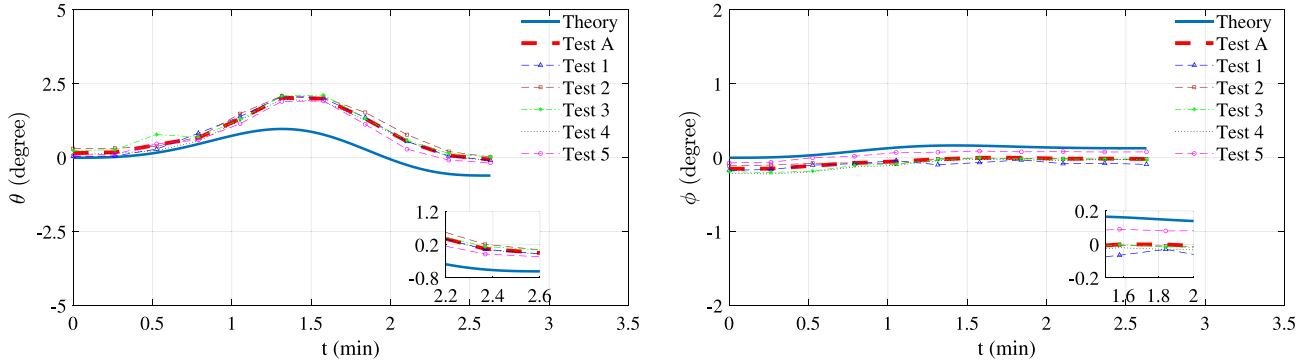

(a) The heel angle comparison (b) The trim angle comparison

Fig. 24. Comparison of theoretical and experimental inclination angles for lifting task LS_{P2}.

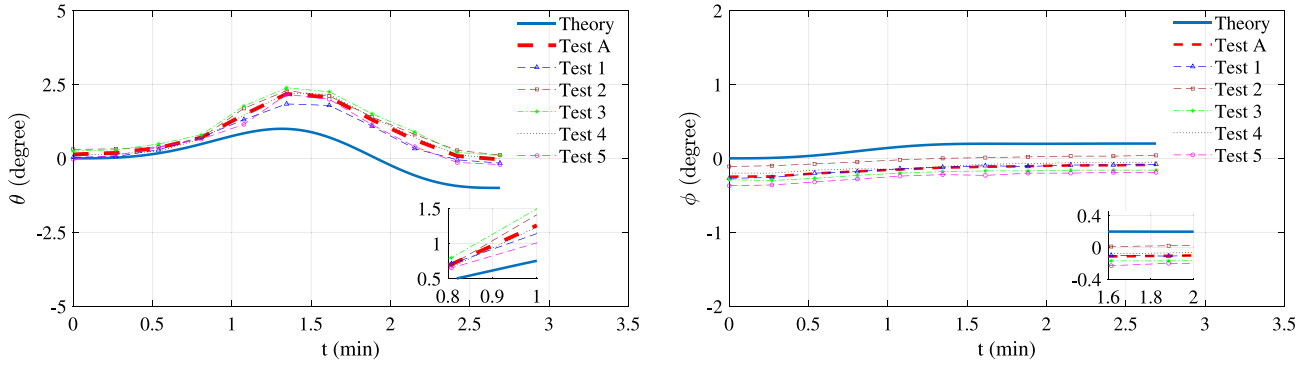

(a) The heel angle comparison (b) The trim angle comparison

Fig. 25. Comparison of theoretical and experimental inclination angles for lifting task LS_{P3}.

Table 10
Operating scenarios regarding different loading masses.

Lifting scenario	Starting position (Rotation angle, Amplitude angle)	Ending position (Rotation angle, Amplitude angle)	Load mass
LS_{M1}	(0°, 20.00°)	(90.00°, 50.00°)	30.00 kg
LS_{M2}	(0°, 20.00°)	(90.00°, 50.00°)	40.00 kg
LS_{M3}	(0°, 20.00°)	(90.00°, 50.00°)	50.00 kg

different target positions and the corresponding short-time characteristic of the CMD method meets the requirements of the intelligent operations.

From the above analysis, it can be concluded that the proposed CMD method can effectively obtain the matching scheme of the lifting trajectory and optimal ballast water allocation for various lifting scenarios regarding different target positions of the lifting activities. Besides, all the schemes meet the safety requirements of the offshore lifting industry. Therefore, the feasibility of the proposed CMD method regarding various lifting target positions can be demonstrated.

5.2.2. Experimental validation regarding different target positions

Based on the numerical results achieved from the CMD method performed in Section 5.2.1, the experimental validation can be further carried out. For the above three lifting scenarios, the obtained lifting trajectory and ballasting water allocation scheme are simultaneously input into the RFC test stand, thereby controlling it to conduct the actual experiments. In order to reduce the experimental error and improve the reliability, the experiment of each lifting scenario is repeated five times. By collecting and processing the real-time data of the lifting experiments, comparisons of the hull inclination between the theoretical and experimental values are illustrated in Figs. 23~25. The thin dotted lines represent the histories of the heel and trim angles obtained from the five repeated lifting experiments, respectively. The thick dotted lines represent the average values of the heel and trim angles obtained by the five repeated experiments, respectively. The theoretical values of the heel and trim angles obtained from the CMD method are represented by thick solid lines.

From Figs. 23~25, it is apparent that both the heel and trim angles of the RFC test stand highly resemble the theoretically optimal inclination angles derived from the CMD method, affirming the ability of the proposed CMD method in providing reliable solutions for practical applications for offshore lifting operations. By close observation, there exists a certain deviation between the theoretical value and the experimental value. A thorough analysis suggests that this deviation may be attributed to inaccurate monitoring of experimental data due to sensor errors, as well as the delay in valve switch and water flow within the pipeline. Generally, such deviations between theoretical and experimental values are common in practical scenarios, and the corresponding deviation in this experiment falls within an acceptable range, thereby not impacting the rationality and validity of the experimental results. Furthermore, the variation ranges of heeling angle and trim angle measured in this actual experiment fully comply with the safety requirements of offshore lifting operations. Based on the aforementioned analysis, the feasibility and reliability of the CMD method in practical applications of offshore lifting activities can be effectively validated.

5.3. Efficacy validation regarding different loading masses

For better comparison, three different loads, including 30 kg, 40 kg, and 50 kg, are selected in this section to perform the actual lifting experiments. In order to eliminate the influence of other factors on the experimental results, the starting and ending positions of the lifting activities are all set to the same. Detailedly, the initial positions for the lifting activities are defined as the center of mass of the load with a horizontal rotation angle of 0° and a boom amplitude angle of 20°, and the final positions for the lifting activities are defined as the center of mass of the load with a horizontal rotation angle of 90° and a boom amplitude angle of 50°. The horizontal rotation angles for these lifting activities are also set to 90°, as this position represents the most critical point in terms of safety and stability. In this way, three different lifting scenarios with different loading masses are formed, as listed in Table 10.

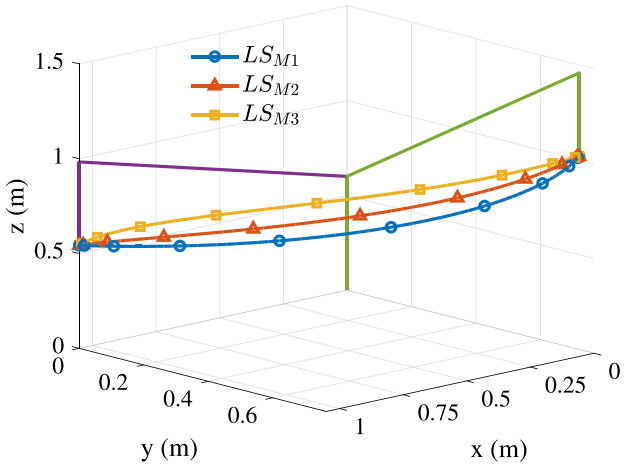

Fig. 26. The optimal lifting trajectories regarding different loading masses obtained from the CMD method.

5.3.1. Numerical validation regarding different loading masses

The CMD method is utilized to find the optimal matching schemes of the lifting trajectory and the ballast water allocation of the RFC test stand regarding different loading masses. The optimal lifting trajectories are presented in Fig. 26, from which it is seen that all the obtained trajectories are continuous and smooth without abrupt changes, conforming to the practical crane controls. In detail, the spatial position of the overall lifting trajectory gradually increases with the loading mass increasing, because the CMD method needs to find the best trajectory to adapt to different ballast water allocation schemes. The corresponding key control parameters of the optimal trajectories are illustrated in Fig. 27. It is seen that the increase of crane loads has slight influences on optimal control parameters, and the rotation speeds of different mechanisms are all smooth and satisfy the constraints. Thus, it can be concluded that the proposed CMD method can find the optimal lifting trajectory between arbitrary loading masses.

Under the premise of fully matching the lifting trajectory, the CMD method achieves the corresponding ballast water allocation schemes according to different loading masses, and the curves are smooth without breaking points, meeting the actual control requirements, as illustrated in Fig. 28. As seen, different numbers of tanks participate in the operation process and the ballast water levels of each tank show different changing trends according to different working conditions of loading masses. The histories of the heel and trim angles of the RFC test stand achieved by the CMD method regarding different loading masses are illustrated from Figs. 29 to 31 (the thick solid lines marked with "Theory"). It is evident that the maximum heel angle and trim angle of

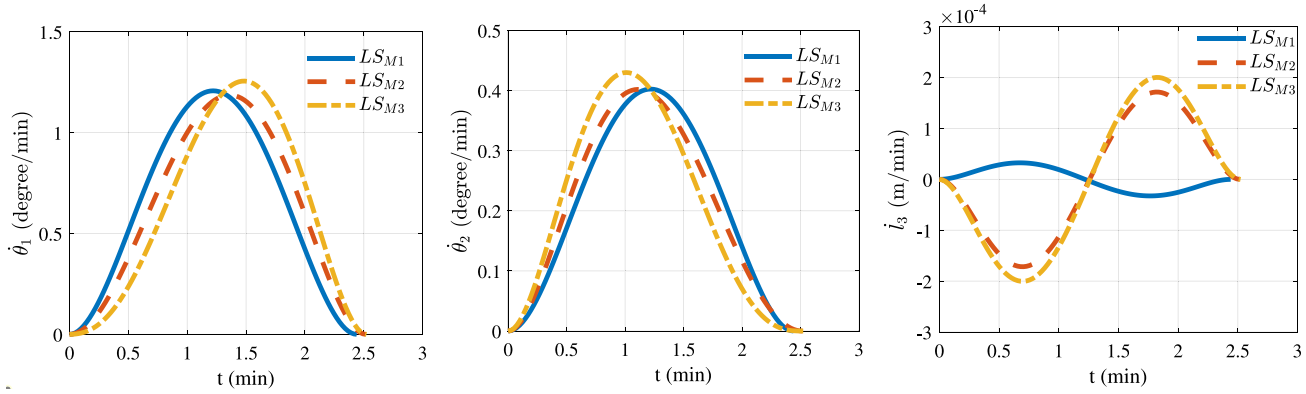

(a) The rotation speed of the crane base (b) The rotation speed of the lifting arm (c) The rotation speed of the rope

Fig. 27. The optimal control parameters obtained from the CMD method regarding different loading masses.

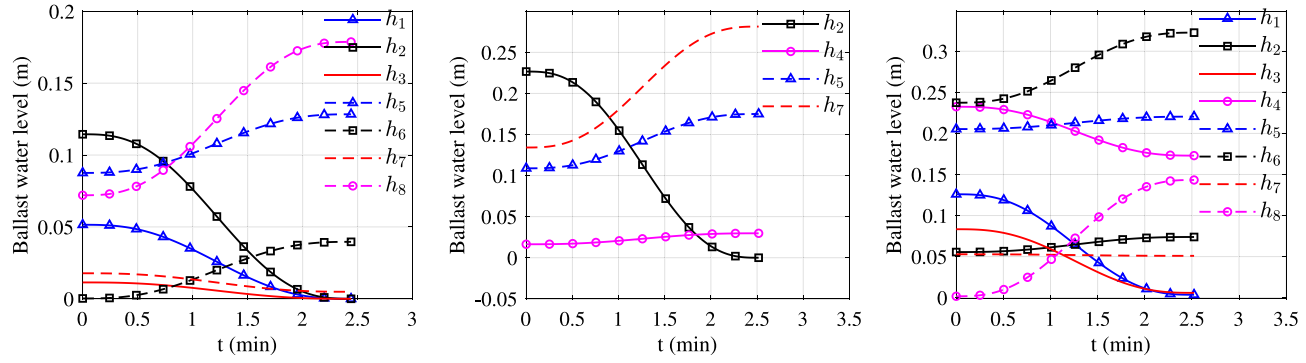

(a) The optimal ballast scheme regarding LS_{M1} (b) The optimal ballast scheme regarding LS_{M2} (c) The optimal ballast scheme regarding LS_{M3}

Fig. 28. The optimal ballast schemes obtained from the CMD method regarding different loading masses.

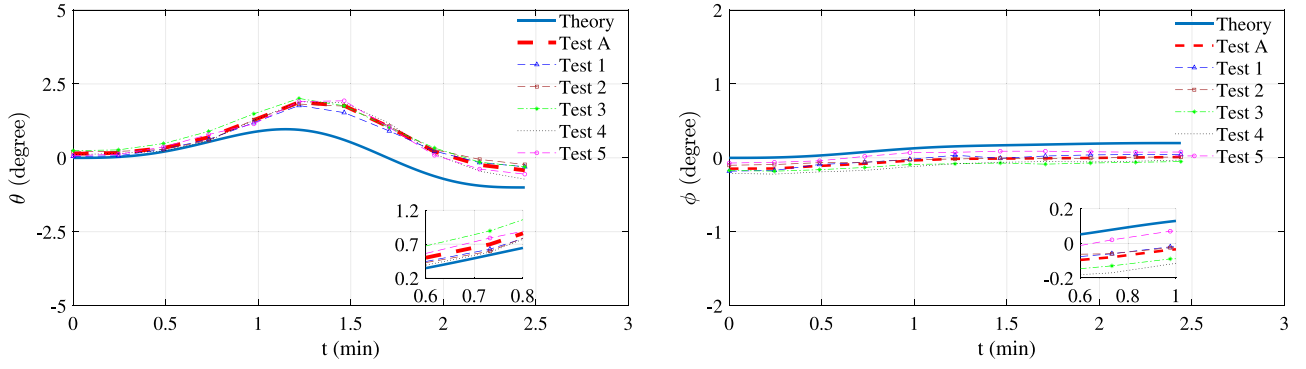

(a) The heel angle comparison (b) The trim angle comparison

Fig. 29. Comparison of theoretical and experimental inclination angles for lifting task LS_{M1}.

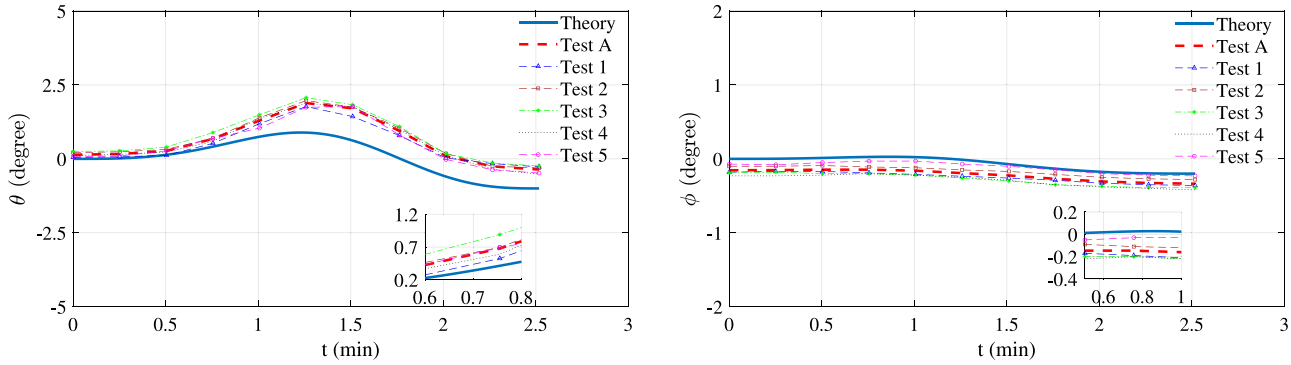

(a) The heel angle comparison (b) The trim angle comparison

Fig. 30. Comparison of theoretical and experimental inclination angles for lifting task LS_{M2}.

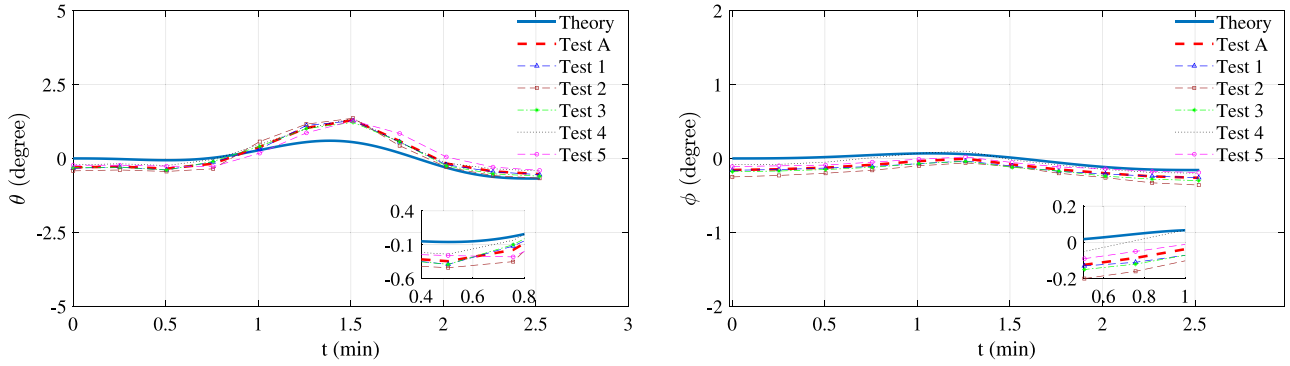

(a) The heel angle comparison (b) The trim angle comparison

Fig. 31. Comparison of theoretical and experimental inclination angles for lifting task LS_{M3}.

Table 11
CMD results comparisons of the RFC test stand regarding different loading masses.

Lifting scenario	LS_{M1}	LS_{M2}	LS_{M3}
Lifting operation time (min)	2.44	2.52	2.52
Total energy consumption (kJ)	17.36	20.69	23.83
Ballast water allocation quantity (kg)	46.66	55.59	63.95
Decision-making time (min)	0.43	0.42	0.45

the RFC test stand are both within the safe range, meeting the industry requirements of the RFC operations.

Table 11 lists the optimization results derived from the proposed CMD method regarding different loading masses. It can be figured out that the lifting operation time, the total energy consumption, and the ballast water allocation quantity all present upward trends with the lifting loading mass increasing. The decision-making time does also meet the requirements of the intelligent operations. To summarize, the CMD method proposed in this study can effectively generate the optimal matching schemes of the lifting trajectory and ballast water allocation for the RFC despite the increase in loading mass. These schemes meet the safety requirements of the relevant industry, thus demonstrating the feasibility of the CMD method in addressing such problems.

5.3.2. Experimental validation regarding different loading masses

Utilizing the numerical results obtained from the CMD method analyzed above in Section 5.3.1, the actual lifting experiments of the RFC test stand is performed. Similarly, the experiment of each lifting scenario is repeated five times to reduce the experimental errors. Figs. 29~31 illustrate the comparisons of the hull inclination between the theoretical and the experimental values by collecting and processing real-time data from the lifting experiments. The meanings represented by different line types are the same as those corresponding to the line types in Figs. 23~25. It is important to note, as mentioned in Section 5.2.2, that the deviations observed in this experiment fall within an acceptable range, thereby not impacting the rationality and validity of the experimental results. From Figs. 29~31, it demonstrates a significant alignment between the inclination angles obtained from the actual experiments and those derived from theoretical calculations. This confirms the practical feasibility and effectiveness of the theoretical scheme generated by the CMD method. Furthermore, the hull remains in a safe state throughout the lifting operation, highlighting the significant advantages of the CMD method in ensuring operational safety.

6. Conclusion and future work

This study addresses the issue of deteriorated quality and safety in offshore lifting operations due to the mismatch of lifting trajectory and ballast water allocation under the current manual operation mode of the revolving floating crane (RFC). To facilitate intelligent upgrade of the RFC operational process, a novel collaborative matching design (CMD) method for the lifting trajectory and ballast water allocation of the RFC is developed based on the point to point (PTP) theory. Based on the relevant theories and experimental studies performed above, following conclusions can be drawn:

(1) The CMD optimization model of RFC lifting trajectory and ballast water allocation is established, which takes the safety maximization, the energy consumption minimization and the efficiency maximization of RFC lifting operations as optimization objectives, and the safety and stability of offshore operations as constraints;

(2) A solution strategy for the CMD method is established based on the concept of time discretization. Solution results reveal that the CMD method outperforms the conventional sequential design (SD) method in terms of the lifting operation time (11.20% reduction), total energy consumption (16.50% reduction), ballast water allocation (17.84% reduction), and decision-making time (54.50% reduction);
(3) To certify the efficacy and feasibility of the proposed CMD method, numerical and experimental validations regarding various lifting scenarios are conducted using the actual RFC test stand. Results demonstrate the theoretical and practical feasibility of the proposed CMD method regarding various working conditions.

Summarily, the proposed CMD method can better meet the safety requirements of the offshore lifting equipment, laying theoretical and methodological foundations for the intelligent development of the RFC and other maritime equipment.

The experimental sections of this study involve the uses of a scaled RFC test stand, which may have variations in size and motion characteristics compared to a real RFC. Therefore, in future work, high-precision modeling techniques (e.g., the digital twins) that can accurately replicate the operational performances of the actual RFC can be utilized in the CMD of operational schemes. In actual operations, waves may affect the safety of offshore lifting and this key issue will be specifically investigated in the future work. Furthermore, for large-scale offshore lifting operations, it may require the collaboration of two or more RFCs, therefore, it is worth exploring the extension of the CMD method for designing the collaborative work schemes of multiple RFCs.

CRediT authorship contribution statement

Xiaobang Wang: Methodology, Resources, Validation, Writing – original draft, Supervision. **Siyu Li:** Investigation, Methodology, Validation, Writing – original draft. **Yang Yu:** Investigation, Validation. **Jie Zhang:** Validation, Writing – original draft. **Zhijie Liu:** Resources, Supervision.

Declaration of competing interest

The authors declare that they have no known competing financial interests or personal relationships that could have appeared to influence the work reported in this paper.

Data availability

Data will be made available on request.

Acknowledgments

This work is supported by National Natural Science Foundation of China (Grant No. 52201406); Doctoral Start-up Foundation of Liaoning Province, China (Grant No. 2021-BS-074); and Fundamental Research Funds for the Central Universities, China (Grant No. 3132023117, 3132023516, 017231017, and 3132023606)

References

Book, W.J., 1984. Recursive Lagrangian dynamics of flexible manipulator arms. Int. J. Robot. Res. 3, 87–101. http://dx.doi.org/10.1177/027836498400300305.

CCS, 2016. CCS rule change notice for: Lifting appliances of ships and offshore installations. https://www.ccs.org.cn/ccswzen/file/download?fileid=201950000000001474. (Accessed 15 September 2023).

Chen, Y., Château, P.A., Chang, Y., 2023. Hybrid multiple-criteria decision-making for bulk carriers ballast water management system selection. Ocean Coast. Manage. 234, 106456. http://dx.doi.org/10.1016/j.ocecoaman.2022.106456.

Chen, J., Lin, Y., Huo, J., Zhang, M., Ji, Z., 2010a. Optimal ballast water exchange sequence design using symmetrical multitank strategy. J. Mar. Sci. Technol. 15, 280–293. http://dx.doi.org/10.1007/s00773-010-0087-9.

Chen, J., Lin, Y., Huo, J., Zhang, M., Ji, Z., 2010b. Optimization of ships' diagonal ballast water exchange sequence using a multiobjective genetic algorithm. J. Ship Res. 54, 257–267. http://dx.doi.org/10.5957/jsr.2010.54.4.257.

CRS, 2011. China Rescue and Salvage of Ministry of Transport of the People's Republic of China, Huatianlong, http://www.crsmot.org.cn/jiulaozb_jlj/201105/t20110513_942947.html. (Accessed 13 January 2024).

Dutta, S., Cai, Y., Zheng, J., 2023. Multi-objective anti-swing trajectory planning of double-pendulum tower crane operations using opposition-based evolutionary algorithm. http://dx.doi.org/10.48550/arXiv.2305.18745, arXiv preprint arXiv:2305.18745.

Fang, Y., Hu, J., Liu, W., Shao, Q., Qi, J., Peng, Y., 2019. Smooth and time-optimal S-curve trajectory planning for automated robots and machines. Mech. Mach. Theory 137, 127–153. http://dx.doi.org/10.1016/j.mechmachtheory.2019.03.019.

Gunnu, G.R., Moan, T., 2018. Stability assessment of anchor handling vessels during operations. J. Mar. Sci. Technol. 23, 201–227. http://dx.doi.org/10.1007/s00773-017-0465-7.

Guo, Z., Cao, Z., Wang, W., Jiang, Y., Xu, X., Feng, P., 2021. An integrated model for vessel traffic and deballasting scheduling in coal export terminals. Transp. Res. E 152, 102409. http://dx.doi.org/10.1016/j.tre.2021.102409.

Hoang, N.Q., Lee, S.G., Kim, H., Moon, S.C., 2014. Trajectory planning for overhead crane by trolley acceleration shaping. J. Mech. Sci. Technol. 28, 2879–2888. http://dx.doi.org/10.1007/s12206-014-0641-1.

Hsu, Y., Huang, M., Fung, R., 2014. Energy-saving trajectory planning for a toggle mechanism driven by a PMSM. Mechatronics 24, 23–31. http://dx.doi.org/10.1016/j.mechatronics.2013.11.004.

Huang, L., Dutta, S., Cai, Y., 2020. Laser scanned real environment for intelligent virtualization of crane lifting. Virtual Real. Intell. Hardw. 2, 87–103. http://dx.doi.org/10.1016/j.vrih.2020.04.003.

Huang, M., Hsu, Y., Fung, R., 2011. Minimum-energy point-to-point trajectory planning for a motor-toggle servomechanism. IEEE/ASME Trans. Mechatronics 17, 337–344. http://dx.doi.org/10.1109/TMECH.2010.2103366.

Jia, Z., Lei, S., 2021. Ballast water allocation optimization of crane vessels based on MOEA/D algorithm. Chin. J. Ship Res. 16, 155–163. http://dx.doi.org/10.19693/j.issn.1673-3185.02049.

Kurniawan, A., Ma, G., 2009. Optimization of ballast plan in launch jacket load-out. Struct. Multidiscip. Optim. 38, 267–288. http://dx.doi.org/10.1007/s00158-008-0287-7.

Li, G., Ma, X., Li, Z., Guo, P., Li, Y., 2023a. Kinematic coupling-based trajectory planning for rotary crane system with double-pendulum effects and output constraints. J. Field Robotics 40, 289–305. http://dx.doi.org/10.1002/rob.22130.

Li, S., Zou, Y., Lai, X., Liu, Z., Wang, X., 2023b. Performance-maximum optimization of the intelligent lifting activities for a polar ship crane through trajectory planning. Proc. Inst. Mech. Eng. C 237, 765–781. http://dx.doi.org/10.1177/09544062221111707.

Liong, S., Kuo, F., Gan, Y., Sheng, Y., Wang, S., 2023. Predicting trajectory of crane-lifted load using LSTM network: A comparative study of simulated and real-world scenarios. Expert Syst. Appl. 228, 120215. http://dx.doi.org/10.1016/j.eswa.2023.120215.

Liu, Z., Jiang, J., Gan, Z., Lin, C., 2022a. Ballast water dynamic allocation optimization model and analysis for safe and reliable operation of floating cranes. Ann. Oper. Res. 311, 279–294. http://dx.doi.org/10.1007/s10479-019-03213-2.

Liu, Z., Jiang, J., Lin, C., Sun, D., 2018. Ballast water high-efficiency allocation optimisation modelling with dynamic programming for revolving floating cranes. Ships Offshore Struct. 13, 857–867. http://dx.doi.org/10.1080/17445302.2018.1470914.

Liu, Q., Lu, Z., Liu, Z., Lin, P., Wang, X., 2022b. Ballast water dynamic allocation optimization for revolving floating cranes based on a hybrid algorithm of fuzzy-particle swarm optimization with domain knowledge. J. Mar. Sci. Eng. 10, 1454. http://dx.doi.org/10.3390/jmse10101454.

Lu, B., Lin, J., Fang, Y., Hao, Y., Cao, H., 2022. Online trajectory planning for three-dimensional offshore boom cranes. Autom. Constr. 140, 104372. http://dx.doi.org/10.1016/j.autcon.2022.104372.

Peng, H., Shi, B., Wang, X., Li, C., 2019. Interval estimation and optimization for motion trajectory of overhead crane under uncertainty. Nonlinear Dynam. 96, 1693–1715. http://dx.doi.org/10.1007/s11071-019-04879-w.

Rams, H., Schöberl, M., Schlacher, K., 2017. Optimal motion planning and energy-based control of a single mast stacker crane. IEEE Trans. Control Syst. Technol. 26, 1449–1457. http://dx.doi.org/10.1109/TCST.2017.2710953.

Rethfeldt, C., Lack, S., Jeinsch, T., 2023. Optimization-based actuator allocation for underwater vehicles with variable buoyancy systems. In: 2023 International Interdisciplinary PhD Workshop. IIPhDW, IEEE, pp. 1–6. http://dx.doi.org/10.1109/IIPhDW54739.2023.10124421.

Tho, H.D., Kaneshige, A., Terashima, K., 2020. Minimum-time S-curve commands for vibration-free transportation of an overhead crane with actuator limits. Control Eng. Pract. 98, 104390. http://dx.doi.org/10.1016/j.conengprac.2020.104390.

Wang, X., Li, S., Liu, Q., Liu, Z., 2022a. Sequential matching optimization for lifting trajectory and ballast water allocation of the intelligent revolving floating crane. Ocean Eng. 266, 113061. http://dx.doi.org/10.1016/j.oceaneng.2022.113061.

Wang, S., Pan, D., Zhou, Z., Yu, H., Ma, X., Fang, G., 2022b. Optimization method and experimental research on attitude adjustment scheme of attitude adaptive rescue robot. Sci. Rep. 12, 18010. http://dx.doi.org/10.1038/s41598-022-22991-7.

Wang, X., Sun, W., Li, E., Song, X., 2018. Energy-minimum optimization of the intelligent excavating process for large cable shovel through trajectory planning. Struct. Multidiscip. Optim. 58, 2219–2237. http://dx.doi.org/10.1007/s00158-018-2011-6.

Wilson, J.C., 2003. Repair of new long-span bridges damaged by the 1995 Kobe earthquake. J. Perform. Constr. Facil. 17, 196–205. http://dx.doi.org/10.1061/(ASCE)0887-3828(2003)17:4(196).

Zhang, Q., Zhang, J.J., He, J., Li, Y.F., Qin, X.R., 2010. A method of dynamic modeling of a large floating crane and its external excitations. Adv. Mater. Res. 139, 2440–2445. http://dx.doi.org/10.4028/www.scientific.net/AMR.139-141.2440.

Zhu, H., Du, Z., Xu, D., Tang, Y., 2020. Optimization solutions for self-propelled modular transporter (SPMT) load-outs based on ballast simulation. Ocean Eng. 206, 107355. http://dx.doi.org/10.1016/j.oceaneng.2020.107355.